*Physics – Uspekhi* **66** (10) 1037 – 1058 (2023) 

*CONFERENCES AND SYMPOSIA*

PACS numbers: 42.55.Lt, **42.60. – v**, **42.62. – b**

*ON THE 100th ANNIVERSARY OF THE BIRTH OF N G BASOV*

# N G Basov's role in the development of excimer lasers: a half-century history from the launch of the first $Xe_2$ laser at the Lebedev Physical Institute to modern laser systems

V D Zvorykin

DOI: https://doi.org/10.3367/UFNe.2022.11.039357

## Contents



**Abstract. In a review dedicated to the 100th anniversary of the birth of academician N G Basov, the fate of one of his scientific predictions is traced: obtaining lasing at bound-free transitions of liquid xenon. Launched at the Lebedev Physical Institute (LPI) of the Academy of Sciences of the USSR in 1970, the $Xe_2$ laser pumped by an electron beam marked a new dimension in laser physics: the advent of high-power excimer lasers generating radiation in the range from visible to vacuum ultraviolet. The main types and excitation methods of excimer lasers and the properties of their gain medium are considered. The most powerful pulsed excimer laser systems designed for laser thermonuclear fusion and amplification of UV multiterawatt ultrashort pulses are described, as well as repetition-rate lasers for applications in medicine, microelectronics, material processing, etc.**

**Keywords:** excimer lasers, operating principles, main types, applications

**V D Zvorykin**
Lebedev Physical Institute, Russian Academy of Sciences,
Leninskii prosp. 53, 119991 Moscow, Russian Federation
E-mail: zvorykin@sci.lebedev.ru

Received 14 April 2023
*Uspekhi Fizicheskikh Nauk* **193** (10) 1103 – 1126 (2023)
Translated by E N Ragozin

## 1. Introduction

Excimer lasers, which appeared in the early 1970s, today occupy a prominent place among other high-power lasers. They exhibit a high output energy in pulsed mode, a high average power in repetition-rate mode, high efficiency, a wide range of lasing wavelengths lying in the visible, ultraviolet (UV), and vacuum ultraviolet (VUV) ranges, and low diffraction-limited radiation divergence. In this regard, excimer lasers attract attention as very promising for laser thermonuclear fusion (LTF), isotope separation, photochemistry, and laser technology for materials processing, communications, microelectronics, medicine, etc. Much attention is paid to them in military programs. Priority research carried out under the leadership of N G Basov at the Laboratory of Quantum Radiophysics of the Lebedev Physical Institute of the USSR Academy of Sciences (FIAN) in 1970–1975 played an important role in understanding the physical processes in excimer lasers on dimers, halides, and oxides of noble gases when excited by an electron beam, electric discharge, and broadband VUV radiation, and contributed to the development of this area of laser technology at many institutes and enterprises in the country. In the United States, within the framework of national programs, lasers with output energies of hundreds and thousands of joules, both pulsed and repetition-rate, were launched by the 1990s. For LTF, scientific and technical projects of repetition-rate KrF laser systems with an output energy up to 1 MJ at a pulse repetition rate of about 10 Hz were developed and partially implemented, and an XeF laser with a pulse repetition rate of hundreds of hertz and an average output power of several kilowatts was

made for military applications. During these years, intensive research on the development of excimer lasers was also carried out in European countries, Japan, and China.

This review was written in memory of the outstanding Soviet and Russian scientist, Nobel laureate in 1964 for the invention of the principles of generation and amplification of induced electromagnetic radiation in lasers and masers, Academician N G Basov (14.12.1922–01.07.2001), the 100th anniversary of whose birth was recently celebrated in our country. The author, who came to the Lebedev Physical Institute in 1971 and was directly involved in the research on excimer lasers at the institute, had the honor of giving a report on the role of N G Basov in this work at the ceremonial meeting of the Department of General Physics and Astronomy of the Russian Academy of Sciences, which was held at the Lebedev Physical Institute on November 28, 2022. This speech formed the basis of this review, which contains a brief excursion into the history of the discovery and subsequent research on excimer lasers and a description of the powerful excimer laser systems made in different laboratories around the world for LTF, ultrashort pulse (USP) amplification, and many other applications. The major contribution of Russian scientists and FIAN to this area of physical research is also presented.

### 1.1 History of discovery: from the initial idea to the first excimer lasers

Excimer lasers today are the most powerful and efficient sources of coherent radiation in the visible, UV, and VUV regions of the spectrum. The generation and amplification of radiation in these lasers occurs at transitions between the excited bound electronic state of the molecule and the repulsive or weakly bound ground state. The fundamental possibility of obtaining lasing from bound-free transitions in $H_2$ and $Hg_2$ was first discussed by F Houtermans in 1960 [1]. In 1966, N G Basov proposed using liquefied noble gases for this purpose [2], with one of which, liquefied xenon, lasing in the VUV region of the spectrum with a wavelength $\lambda = 176$ nm was first obtained in 1970 [3, 4]. The practical implementation of the idea became possible due to the use of a powerful relativistic electron beam for pumping. It was not long before lasing was obtained on $Xe_2$ dimers with $\lambda = 173$ nm in gaseous xenon compressed to several atmospheres [5, 6], and then on other dimers: $Kr_2$ with $\lambda = 146$ nm [7] and $Ar_2$ with $\lambda = 126$ nm [8] — the shortest wavelength of excimer lasers today.

### 1.2 Main types and methods of pumping excimer lasers

The name 'excimer' comes from the abbreviation 'excited dimer' and was originally used for diatomic homonuclear molecules. More recently, it received a broader interpretation, and currently a very broad class of molecules is called excimers, including heteronuclear diatomic and polyatomic molecules of noble gas halides ArF, ArCl, KrF, KrCl, $Ar_2F$, $Kr_2F$, ArKrF, etc., as well as oxides of noble gases. Excimers sometimes include metal halides HgI, HgBr, HgCl, CdI, as well as halogens and interhalogens $F_2$, $Cl_2$, $Br_2$, ClF. Laser transitions in these molecules occur from the vibrational levels of the bound excited electronic state of the molecules to the lower repulsive state or to the highly excited vibrational levels of the lower bound electronic state. In both cases, the lower laser state is rapidly depopulated due to either molecule dissociation or vibrational relaxation.

The parameters of excimer molecules, the systematics of terms and potential energy diagrams for different electronic states, and the kinetics of plasma-chemical reactions occurring during pumping of the medium and during laser oscillation (or radiation amplification) are given in a number of reviews and books (see, for example, Refs [9–15]). Although the launch of the first lasers on noble gas dimers was of fundamental importance, their subsequent development was limited to the development of relatively small laboratory samples intended for physical research in the VUV region of the spectrum. The highest output power of an $Xe_2$ laser, 60 MW per pulse of 20 ns in duration with a specific energy output of 6 J $l^{-1}$, was obtained in Ref. [16]. Scaling of these lasers encounters major difficulties, mainly associated with the need for very high pump powers and the lack of high-quality optical elements in the VUV range.

A new and important avenue in excimer lasers was opened by research carried out in 1974–1976 [17–23], during which the high efficiency of excitation transfer from noble gases to halides was demonstrated and lasers on noble gas halides were launched: XeF with $\lambda = 353$ nm [19], KrF with $\lambda = 248$ nm, XeC with $\lambda = 308$ nm [20], XeBr with $\lambda = 282$ nm [21], ArF with $\lambda = 193$ nm [22], and KrCl with $\lambda = 222$ nm [23]. In all these cases, an electron beam was used for pumping. Almost simultaneously, other methods of exciting these lasers were implemented: electroionization, i.e., a non-self-sustained electric discharge supported by an electron beam [24] and various versions of a self-sustained electric discharge without preionization [25, 26] and with preionization by UV radiation [27]. Later, X-rays [28] and neutron radiation from a nuclear reactor [29] were used for preionization. Pumping of excimer media was also carried out by beams of protons [30] and heavy multiply charged ions [31, 32], and radio frequency [33] and microwave discharges [34, 35]. Optical pumping of excimer lasers with broadband radiation from an excimer lamp [36, 37] and an open high-current discharge [38–40] has been used to advantage. More recently, it has been possible to obtain lasing in cryogenic XeF crystals at $D \rightarrow X$, $B \rightarrow X$, and $C \rightarrow A$ transitions under coherent optical pumping [41, 42]. Thus, excimer lasers benefit from a wide range of lasing wavelengths, extending from the far VUV to the visible region of the spectrum, and a wide variety of excitation methods.

The highest intrinsic efficiency, which is understood as the ratio of output laser energy to pump energy, and specific lasing energy were obtained for excimer lasers on noble gas halides excited by an electron beam (Table 1) [43]. Ranking highest in this respect is the KrF laser, which has an efficiency of 10–12% with an energy output of 10–20 J per liter of gain medium. For discharge-pumped lasers, these values are somewhat lower: the efficiency is 2.5–2.6%, and the specific output energy is 2.4–3.0 J $l^{-1}$.

Another important advantage of electron beam excitation is the potentiality to scale excimer lasers to very large sizes,

**Table 1.** Efficiency and specific output energy of noble gas halide lasers pumped by an electron beam.

| Laser type | Efficiency, % | Specific energy, J $l^{-1}$ |
|---|---|---|
| ArF | 4 – 8 | 10 – 15 |
| KrF | 10 – 12 | 10 – 20 |
| XeCl | 4 – 7 | 5 |
| XeF | 5 | 14 |

which was demonstrated during the first decade after their invention. While the first lasers with a gain medium volume of tens or hundreds of cubic centimeters generated pulses with an energy of less than 1 J, even by 1985 an energy of 10 kJ was obtained from the final module of the multi-stage KrF Aurora facility, which had a volume of 2 $m^3$ and was equipped with a suboptimal unstable resonator [44, 45]. Developed at the same time was a detailed project of the Polaris excimer module with a gain volume of 13 $m^3$, which was designed for an output energy of 100 kJ [46, 47].

Among discharge-pumped excimer lasers, the highest output energy of 66 J in 180-ns-long pulses was obtained from an XeCl laser with X-ray preionization of the gain volume of 22 l at a working mixture pressure of 5 atm with an efficiency of 0.8% [48]. Further scaling of discharge-pumped lasers was limited by the problem of discharge stability in a large gas volume.

Simultaneously with progress in the technology of generating powerful electron beams, systems for circulation working gas mixtures through a laser chamber were improved, which was necessary for cooling the gas in pulse repetition mode. As a result, repetition-rate XeF lasers with a closed gas-dynamic circuit and electron beam pumping were launched to yield average output powers of over 4 kW at a pulse repetition rate of up to 100 Hz [49]. The duration of the laser pulse train in such lasers was about 1 s and was limited by the destruction of the foil used to extract the electron beam from the accelerator into the laser chamber.

The development of the discharge-pumped technique led to the emergence of reliable excimer lasers with a long service life, which ensured their widespread use in medicine, microelectronics, photolithography and other fields. Developed for various technological applications related to cutting, welding, hardening of materials, and industrial production of microchips were excimer lasers with an average output power of over 1 kW at a pulse repetition rate of 100–1000 Hz [50, 51].

## 2. KrF lasers pumped by an electron beam

### 2.1 Properties of the gain medium

A huge number of studies are devoted to kinetic processes and the measurement of the rate coefficients of plasma-chemical reactions in the gain medium of excimer lasers, which we have omitted in this review, since most of these results can be found in the papers mentioned above [9–15]. The KrF laser, which has the highest efficiency and high specific output parameters, is especially attractive for scaling and use as a driver for LTF, amplification of ultrashort pulses, and other applications that require high energies or peak powers of UV radiation. For numerical simulation of a large-volume KrF laser pumped by a relativistic electron beam, A G Molchanov at the Lebedev Physical Institute developed a program [14] that takes into account more than 100 different plasma-chemical reactions among several dozen components, which uses the entire set of experimental and theoretical data on reaction rate coefficients and cross sections. In what follows, when describing the kinetic processes and gain medium of the KrF laser, we adhere to a simplified version of this theoretical model, which nevertheless correctly reflects the specifics of the laser.

The gain medium of a KrF laser pumped by an electron beam usually contains 0.2–0.6% molecular fluorine $F_2$ or

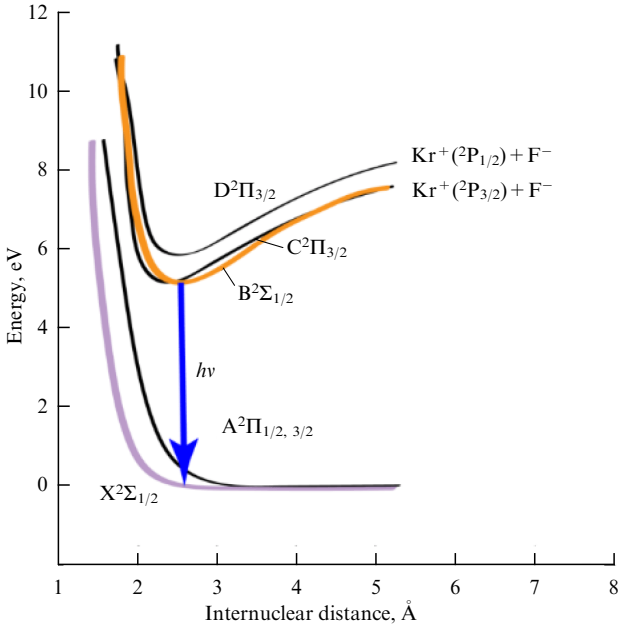


**Figure 1.** Potential curves of lower electronic states of the KrF molecule.

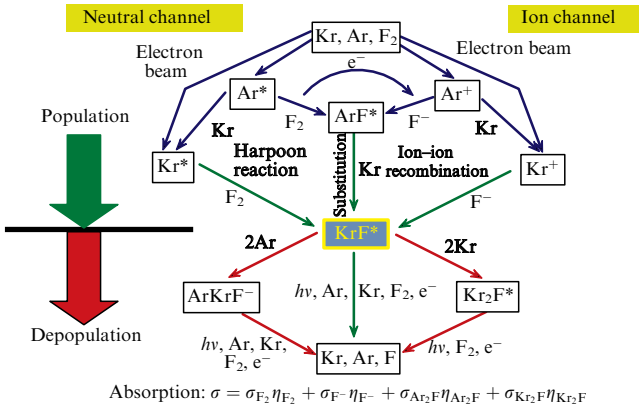


**Figure 2.** Basic kinetic processes in the formation of population inversion in a KrF laser.

some other donor, for example, $NF_3$, 5–10% Kr krypton, and an Ar buffer gas with a total mixture pressure of 1–3 atm. When the electron beam is decelerated in the working gas, a cascade of secondary electrons $e^-$ is formed, whose collision with Ar and Kr atoms produces $Ar^+$ and $Kr^+$ ions and approximately the same number of atoms in various excited states, $Ar^*$, $Ar^{**}$, $Kr^*$, and $Kr^{**}$, where $*$ denotes the set of lower excited states of the 4s electron shell in Ar and 5s in Kr, and $**$ refers to the excited states of Ar and Kr in the 4p and 5p states, respectively. Figure 1 shows a diagram of potential curves for the lowest bound electronic state of the $KrF^*$ molecule $B^2\Sigma_{1/2}$, for $C^2\Pi_{3/2}$ and $D^2\Pi_{3/2}$, close to it in energy, as well as the for ground and first excited repulsive states $X^2\Sigma_{1/2}$ and $A^2\Pi_{1/2,3/2}$. The population of the entire set of bound states of $KrF^*$ occurs through two main channels, so-called neutral and ionic, a simplified diagram of which is shown in Fig. 2. In the neutral channel, excited $Ar^*$ and $Kr^*$ atoms, produced in the collision of secondary electrons with noble gas atoms (reaction 1), subsequently make up excited excimers $ArF^*$ and $KrF^*$ in a harpoon reaction (2) with $F_2$

molecules:

$$e^- + Ar \to Ar^* + e^-, \quad e^- + Kr \to Kr^* + e^-, \tag{1}$$

$$Ar^* + F_2 \to ArF^* + F, \quad Kr^* + F_2 \to KrF^* + F. \tag{2}$$

In the ion channel, reactions occur of noble gas ionization (3) and dissociative attachment of electrons to fluorine molecules (4), followed by the formation of excimers during ion–ion recombination (5):

$$e^- + Ar \to Ar^+ + 2e^-, \quad e^- + Kr \to Kr^+ + 2e^-, \tag{3}$$

$$e^- + F_2 \to F^- + F, \tag{4}$$

$$Ar^+ + F^- \to ArF^*, \quad Kr^+ + F^- \to KrF^*. \tag{5}$$

In the substitution reaction (6), excited $KrF^*$ molecules are produced from $ArF^*$, which is higher in energy:

$$ArF^* + Kr \to KrF^* + Ar. \tag{6}$$

Since the energy gap between the minima of the potential curves for states B and C is a small value, $\Delta E_{BC} = E_B - E_C \approx \pm 200$ cm$^{-1}$ comparable to vibrational quanta, the upper vibrational levels of both electronic states are mixed due to rapid vibrational-rotational energy exchange between these states. The laser transition occurs from a limited number of vibrational levels of the B-state to the repulsive ground state of the X molecule, whose decay produces the initial Kr atoms and atomic fluorine F. Since the rate coefficient for the reduction of the latter into the $F_2$ molecule in the reaction

$$F + F + M \to F_2 + M, \quad M = Ar, Kr \tag{7}$$

is very small ($\sim 10^{-34}$ cm$^6$ s$^{-1}$), the characteristic recovery time of molecular fluorine of $\sim 10^{-3}$ s is far longer than the typical times of electron beam laser pumping $\tau_p = 100-500$ ns, the generation or amplification of laser radiation is possible only in a pulse mode. However, in this case, too, it is necessary to set the initial density of $F_2$ taking into account its 'burn-up,' whose rate increases in proportion to the specific pump power $W$.

The radiative lifetime of the B → X laser transition of a KrF molecule $\tau_r = 6.5$ ns. Taking into account the depopulation of the upper laser state during collisions of an excited $KrF^*$ (B) molecule with electrons and noble gas atoms (see Fig. 2), the lifetime decreases to $\tau_c \approx 2$ ns. The pump power transmitted through the ion and neutral channels (1)–(6) to the B-state minus all other processes that bypass this state, $W_p = \eta_p W$, is proportional to the specific power, where $\eta_p$ is the pump efficiency. According to numerical simulations [14], under optimal conditions, $\eta_p \approx 0.25$. The density of excited particles in the excited state $N^* = \eta_p W \tau_c / h\nu$ is determined by the ratio of population and decay rates, where $h\nu = 5$ eV is the energy of the laser photon. The short lifetime $\tau_c$ does not permit storing population inversion in the gain medium as, for example, in solid-state lasers, and requires a high specific pump power $W \sim 1$ MW cm$^{-3}$ to obtain the required density $N^*$ of excited particles in the upper laser state. The corresponding small signal gain $g_0 = \sigma N^*$, where $\sigma = 2.5 \times 10^{-16}$ cm$^2$ is the stimulated emission cross section.

Important laser parameters are the saturation intensity of the gain medium $I_s = h\nu/\sigma\tau_c \approx 1$ MW cm$^{-2}$ and the saturation energy density $Q_s = h\nu/\sigma = 2$ mJ cm$^{-2}$. The former

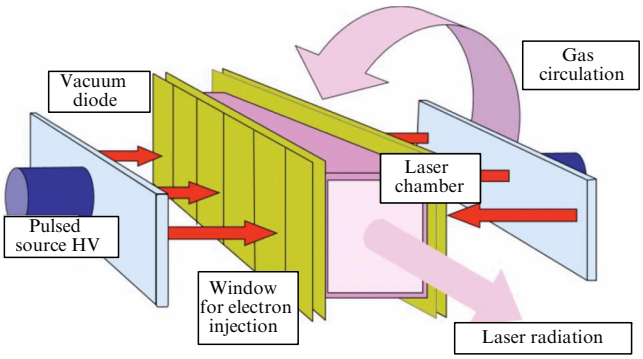


**Figure 3.** Schematic representation of an excimer laser with circulation of the working mixture and bilateral transverse pumping by electron beams. (Adapted with permission, © The Optical Society [81].)

determines the efficiency of the laser in a quasi-stationary lasing mode or when amplifying 'long' pulses with a duration $\tau \geqslant \tau_c$, and the latter determines the efficiency of amplifying 'short' pulses with a duration $\tau \leqslant \tau_c$. In its physical meaning, $I_s$ means the laser intensity $I$, at which the probability of the induced transition $I\sigma/h\nu$ becomes equal to the total depopulation probability of the upper laser level due to radiative decay and collisional quenching $1/\tau_c$. The gain $g(I) = g_0/(1 + I/I_s)$; in this case, $g(I_s) = g_0/2$ is halved compared to $g_0$. In turn, $Q_s$ characterizes the energy $N^* h\nu = (g_0/\sigma)h\nu = g_0 Q_s$ stored in the upper laser level. Since the saturation parameters in a KrF laser are three orders of magnitude smaller than in solid-state lasers, to obtain about the same output energy calls for increasing the KrF laser aperture by the same factor, which can be done if relativistic electron beams with particle energies of 300–600 keV are used for pumping.

In the transverse pump geometry typical of large amplifiers (Fig. 3), beams are introduced into the laser chamber perpendicular to the optical axis from two or more sides, and the electron range, determined by their energy and the pressure of the working gas, is chosen approximately equal to the transverse size of the chamber. Since the average energy spent on the ionization of one Ar atom is 26.4 eV and for Kr is 23.9 eV, the number of secondary electrons produced by one fast electron reaches $\sim 2 \times 10^4$. Although the fraction of electron bremsstrahlung does not exceed 0.5%, together with scattered electrons, it leads to radiation damage to windows — a partial loss of their transparency due to the formation of structural defects and long-lived color centers [52, 53]. A magnetic field applied along the direction of the electron beam almost completely eliminates scattered electrons, but does not eliminate X-ray irradiation of the windows [54].

Another important parameter of the gain medium is the absorption of laser radiation by different initial and intermediate components. The total photoabsorption cross section averaged over the main absorbing components,

$$\sigma_{ph} = \sigma_{F_2}\delta_{F_2} + \sigma_{F^-}\delta_{F^-} + \sigma_{Ar_2F}\delta_{Ar_2F} + \sigma_{Kr_2F}\delta_{Kr_2F}, \tag{8}$$

where $\sigma_i$ are the cross sections for different components ($i = F_2$, $F^-$, $Ar_2F$, $Kr_2F$) and $\delta_i$ are their relative densities. The latter change during pumping and lasing. Thus, the content of molecular fluorine in the gain medium decreases due to the burnup effect, and that of all other components

increases approximately in proportion to the specific pump power. The photoabsorption of $F_2$ near laser windows, where there is no pumping, can be reduced by shortening the distance from the beam boundaries to the windows in the laser chamber, although this increases the rate of their degradation [54]. Since the density of most components depends only slightly on the laser radiation intensity, their associated absorption coefficient $\alpha$ does not saturate even at high intensities. The exception is the excited molecules of the ternary excimer $Kr_2F^*$ produced in collisional quenching of the upper KrF (B) laser level. The associated absorption coefficient saturates with increasing intensity, since the induced transition probability increases compared to collisional quenching (see Fig. 2).

### 2.2 Quasi-stationary amplification of long pulses

Detailed kinetic calculations [14] suggest that the characteristic settling time for amplification and absorption in the gain medium is $\sim 20$ ns. This is significantly shorter than typical durations of electron beam pumping $\tau_p$ and allows us to consider the laser operating mode as quasi-stationary. In the practically important case $I \geqslant I_s$, when saturable absorption can be neglected, the transfer equation for the radiation intensity is of the form

$$\frac{dI}{dx} = I(x)\left(\frac{g_0}{1+I/I_s} - \alpha\right). \tag{9}$$

From Eqn (9), it follows that the limiting value of intensity $I_{max} = I_s[(g_0/\alpha) - 1] \approx I_s(g_0/\alpha)$, since $g_0/\alpha \gg 1$ is achieved for $dI/dx = 0$, i.e., when all generated radiation is absorbed in the gain medium itself and the efficiency of radiation extraction $\eta_{ext}$ is zero. The local value $\eta_{ext}$ is determined by the ratio of the power extracted from a unit volume of the gain medium to the specific pump power arriving at the upper laser level:

$$\eta_{ext} = \frac{dI/dx}{W_p} = \frac{I}{I_s}\left(\frac{1}{1+I/I_s} - \frac{\alpha}{g_0}\right), \tag{10}$$

where $W_p = g_0 I_s$. The optimal intensity

$$I_{opt} = I_s\left[\left(\frac{g_0}{\alpha}\right)^{1/2} - 1\right]$$

corresponds to the maximum value

$$(\eta_{ext})_{max} = \left[1 - \left(\frac{g_0}{\alpha}\right)^{1/2}\right]^2.$$

Since both $g_0 \propto W$ and $\alpha \propto W$, their ratio $g_0/\alpha$ depends only slightly on the pump power $W$ (Fig. 4). For different mixtures and pressures of the working gas, the value of this ratio lies in the range $g_0/\alpha = 10-20$, which corresponds to $(\eta_{ext})_{max} = 0.5-0.6$ with $I_{opt} = (2.2-3.5)I_s$, where $I_s$ also weakly depends on the pump power and amounts to $I_s \approx 1-2$ MW cm$^{-2}$ for typical values of $W \sim 1$ MW cm$^{-3}$. The highest intrinsic efficiency of the laser without inclusion of vibrational relaxation in excited B- and C-electronic states reaches $\eta = \eta_p \eta_{ext} \approx 0.15$. However, the finite relaxation rate reduces this figure to $\eta \approx 0.12$ [14].

Another important factor affecting the efficiency and parameters of a KrF laser is amplified spontaneous emission (ASE). A gain medium with a short radiation

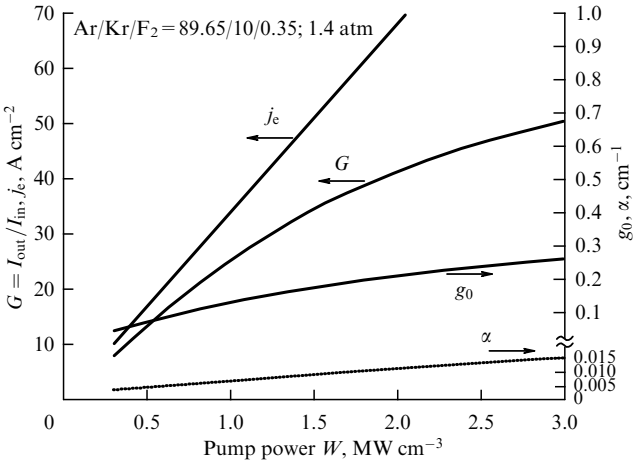


**Figure 4.** Calculated dependences of small signal gain $g_0$, absorption coefficient $\alpha$, and single-pass gain $G = I_{out}/I_{in}$ for the GARPUN amplifier at specific pump power $W$. Working mixture $Ar/Kr/F_2 = 89.65/10/0.35\%$ at a pressure of 1.4 atm; $j_e$ is the current density of the electron beam on each side.

decay time of the upper laser level has a high spontaneous emission power $W_{sp} = h\nu N^*/\tau_r = \eta_p W \tau_c/\tau_r$ with an efficiency $\eta_{sp} = \eta_p \tau_c/\tau_r \approx 0.08$ relative to the specific pump power. ASE propagating along a KrF amplifier saturates the gain medium along with the useful signal. In amplifiers with a high aspect ratio of the aperture to the length, ASE also occurs in the transverse direction. To calculate the parameters of the amplifier, which most often has the shape of a rectangular parallelepiped, in the numerical model [14], the space around each calculation point inside the gain medium was divided into six solid angles based on the sides of the parallelepiped. A system of six radiation transfer equations for the so-called ASE waves $Y_{1...6}$, averaged over the corresponding solid angles, and two equations for longitudinal signal waves propagating towards each other along the axis of a two-pass amplifier was solved, together with equations describing kinetic processes in the gain medium and photoabsorption. This method is also applicable for calculating the contrast of the output signal in terms of laser output power or energy relative to ASE propagating in the same direction.

Figure 5 shows the experimental dependence of the output intensity $I_{out}$ on the input one $I_{in}$, obtained for single-pass amplification of 20-ns pulses in a GARPUN laser with an aperture area of 250 cm$^2$ and a length of 1 m [55], as well as the calculated dependences $I_{out}(I_{in})$ with and without ASE inclusion for various pump powers $W = 0.65$ and 1.3 MW cm$^{-3}$. One can see that ASE reduces the gain $G \equiv I_{out}/I_{in}$ several-fold. Figure 6 shows the calculated dependences $I_{out}(I_{in})$ for two-pass GARPUN amplifier, as well as intrinsic efficiency $\eta = \eta_p \langle \eta_{ext} \rangle$, where

$$\langle \eta_{ext} \rangle = \frac{1}{L}\int_0^L \eta_{ext}(x)\,dx = \frac{I_{out} - I_{in}}{g_0 L} \tag{11}$$

is the efficiency of radiation extraction from the gain medium averaged over the length of the amplifier with the inclusion of ASE. One can see that changing the specific pump power by half, from $W = 1$ to 2 MW cm$^{-3}$, in saturation mode approximately doubles the gain $G$, but entails a decrease in the amplifier efficiency $\eta$ from 10 to 7%.

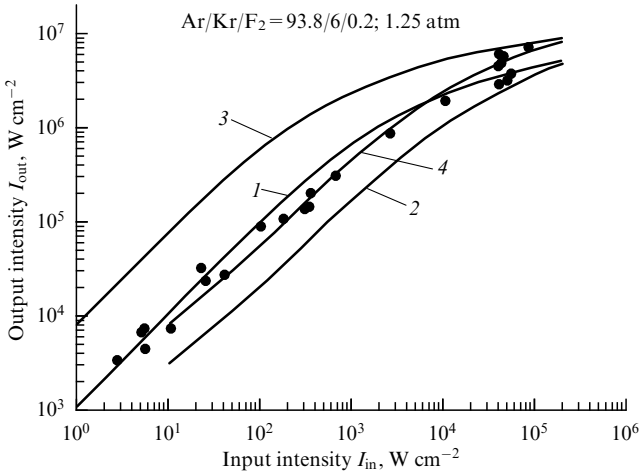


**Figure 5.** Comparison of the experimental dependence of output intensity $I_{out}$ on input intensity $I_{in}$ in a single-pass GARPUN amplifier (points) with numerical simulation for specific pump power $W = 0.62$ MW cm$^{-3}$ without taking into account (*1*) and taking into account ASE (*2*); for pump power $W = 1.3$ MW cm$^{-3}$ without taking into account (*3*) and taking into account ASE (*4*). Working mixture $Ar/Kr/F_2 = 93.8/6/0.2\%$ at a pressure of 1.25 atm.

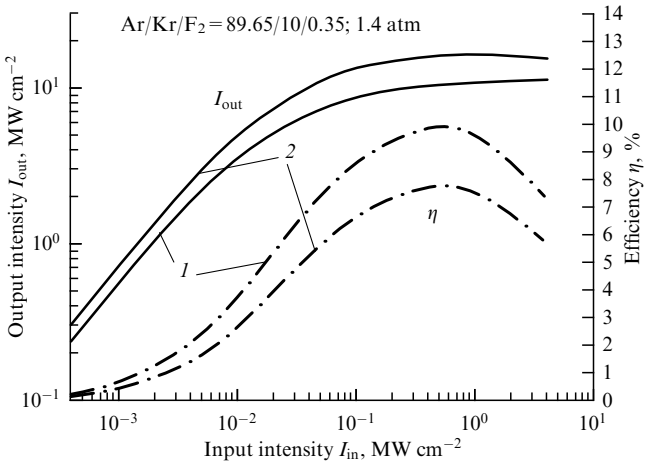


**Figure 6.** Calculated output intensity $I_{out}$ and amplification efficiency $\eta$ in relation to input intensity $I_{in}$ for two-pass GARPUN amplifier for different specific pump powers $W = 1$ (*1*) and 2 MW cm$^{-3}$ (*2*). Working mixture $Ar/Kr/F_2 = 89.65/10/0.35\%$ at a pressure of 1.4 atm.

Figure 7 shows the spatial distributions of ASE in GARPUN KrF laser for single-pass and double-pass amplification schemes in the absence of an input signal at pump power $W = 0.6$ MW cm$^{-3}$ [55]. In this case, a totally reflecting mirror returns the radiation to the amplifier, doubling the effective amplification length. In the single-pass configuration (a), in accordance with formula (9) under the condition $Y_{3,4} \ll I_s$, ASE increases according to the exponential law $Y_{3,4}(x) \propto W_{sp} \exp[(g_0 - \alpha)x]$ in the same way in both directions along the length of the amplifier; its influence on the gain of the medium is still relatively small: $g(x) = 0.045-0.055$ compared to $g_0 = 0.08$ cm$^{-1}$. In the two-pass scheme (b), the ASE intensity $Y_4$ reflected from the totally reflecting mirror quickly reaches saturation of the medium ($Y_4 > I_s$) and then increases linearly along the amplifier. This leads to a strong decrease in the gain coefficient: at the output its value drops four-fold compared to $g_0$.

Since in many practically important cases, for example, for LTF, laser pulses with a duration $\tau \sim 10$ ns are required, and the gain medium of a KrF laser does not allow energy to be accumulated for times longer than $\tau_c \approx 2$ ns, an optical angle multiplexing scheme is used for effective amplification of the required pulses with pump duration $\tau_p = 100-500$ ns [56, 57]. The radiation from the master oscillator is divided into many independent beams $N = \tau_p/\tau$, between which a time delay $\Delta\tau \approx \tau$ is introduced, so that a pulse train with total duration $\tau_p$ is quasi-continuously amplified in the amplifier stages. Since all pulses propagate in independent beams spaced angularly apart, it is possible to add them on the target in the required combination by compensating for delays in the optical demultiplexer. Although this complex configuration requires a large number of mirrors and other optical elements, it has a number of advantages discussed in Section 3.1: for example, the highest uniformity of target irradiation for LTF.

### 2.3 Amplification of short pulses and their trains

Incoherent amplification of short pulses with duration $\tau \ll \tau_c$ is described by the modified Frantz–Nodvik equation [58]:

$$\frac{d\varepsilon}{dx} = g(x)\left(1 - \exp(-\varepsilon)\right) - \alpha_{ns}\varepsilon\,, \quad \varepsilon = \frac{Q}{Q_s}\,, \qquad Q(x) = \int_0^\tau I(x,t')\,dt'\,, \tag{12}$$

where $I(x,t)$ and $Q(x)$ are the intensity and energy density of the pulse as it propagates along the amplifier. The gain profile

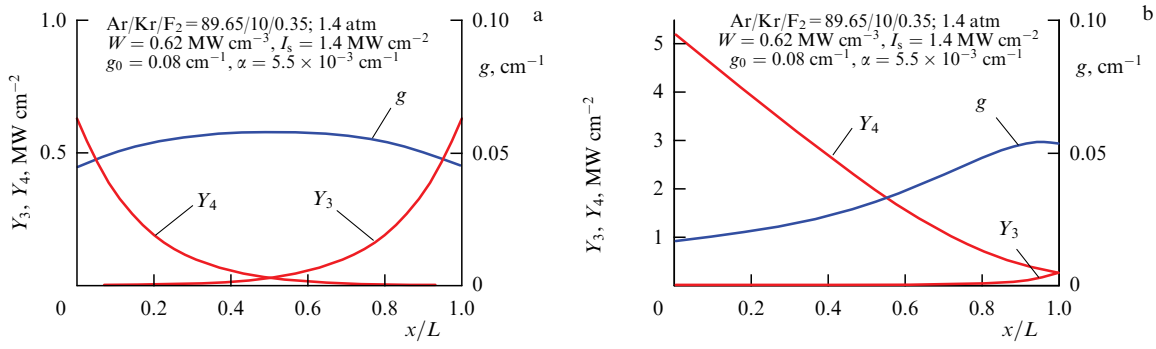


**Figure 7.** Calculated ASE distributions along the axis of a GARPUN amplifier in single-pass (a) and double-pass (b) configurations for a specific pump power $W = 0.62$ MW cm$^{-3}$ ($g_0 = 0.08$ cm$^{-1}$, $\alpha = 5.5 \times 10^{-3}$ cm$^{-1}$, $I_s = 1.4$ MW cm$^{-2}$). Working mixture $Ar/Kr/F_2 = 89.65/10/0.35\%$ at a pressure of 1.4 atm.

$g(x)$ is formed by ASE (see Fig. 7) or a long laser pulse, amplified simultaneously with the short one [55]. This setup, which we proposed in Ref. [59], allows us to reduce losses associated with ASE (see Section 2.4).

Local efficiency of energy extraction from a gain medium by a single short laser pulse $\eta_{1\,\mathrm{ext}}$ is found as the ratio of the increment in energy density per unit amplifier length $\mathrm{d}Q/\mathrm{d}x = Q_\mathrm{s}\,\mathrm{d}\varepsilon/\mathrm{d}x$ to the energy stored in the upper laser level $N^*h\nu = (g_0/\sigma)h\nu = g_0 Q_\mathrm{s}$. In view of Eqns (12), we obtain an expression for $\eta_{1\,\mathrm{ext}}$ along the amplifier length:

$$\eta_{1\,\mathrm{ext}}(x) = \frac{1}{g_0}\left[g(x)\left(1-\exp\left(-\varepsilon\right)\right) - \alpha_{ns}\varepsilon\right]. \tag{13}$$

The maximum $\eta_{1\,\mathrm{ext}}$ value is reached for $\varepsilon_\mathrm{opt} = \ln\left(g/\alpha_{ns}\right)$,

$$\left(\eta_{1\,\mathrm{ext}}\right)_\mathrm{max} = \frac{g}{g_0}\left[1-\frac{\alpha_{ns}}{g}\left(1+\ln\frac{g}{\alpha_{ns}}\right)\right]_\mathrm{max}, \tag{14}$$

and the average efficiency of energy extraction from an amplifier of length $L$ is found by the formula

$$\left\langle\eta_{1\,\mathrm{ext}}\right\rangle = \frac{1}{L}\int_0^L \eta_{1\,\mathrm{ext}}(x)\,\mathrm{d}x = \frac{\varepsilon(L)-\varepsilon(0)}{g_0 L}. \tag{15}$$

To estimate the characteristic efficiency values, assuming $g(x) \equiv g_0$ in the simplest case, from expression (14) we obtain the highest efficiency of energy extraction by a single pulse,

$$\eta_{1\,\mathrm{ext}} = 1-\frac{\alpha_{ns}}{g_0}\left(1+\ln\frac{g_0}{\alpha_{ns}}\right) = 0.7-0.8,$$

for the optimal pulse energy density $Q_\mathrm{opt} = Q_\mathrm{s}\ln\left(g_0/\alpha_{ns}\right) = 4.6-6.0$ mJ cm$^{-2}$. To find the amplification efficiency of a short pulse relative to the entire pump energy, we do well to bear in mind that a single pulse extracts energy from the gain medium accumulated over a time $\tau_\mathrm{c} \sim 2$ ns, which is short compared to the characteristic duration of electron beam pumping $\tau_\mathrm{p}$. As a result, we find that the amplification efficiency of a single short pulse with respect to the pump $\eta_1 = (\tau_\mathrm{c}/\tau_\mathrm{p})\eta_{1\,\mathrm{ext}}\eta_\mathrm{p} \approx 0.004$ is small compared to the efficiency of quasi-stationary amplification of long pulses $\eta = 0.12$ (see Section 2.2).

Since for $\tau_\mathrm{c} \ll \tau_\mathrm{p}$ the accumulation of excited KrF molecules on the upper laser level is impossible, effective energy removal should be carried out by a train of pulses spaced from each other by a time on the order of the lifetime of the excited state $\Delta t \sim \tau_\mathrm{c}$. In this case, for a uniform initial gain profile $g(x) \equiv g_0$, the gain for each of the subsequent pulses does not have time to fully recover after the amplification of the previous pulses and turns out to be less than in the amplification of a single pulse [59, 60]:

$$g_{\Delta t} = g_0\,\frac{1-\exp\left(-\Delta t/\tau_\mathrm{c}\right)}{1-\exp\left(-\varepsilon\right)\exp\left(-\Delta t/\tau_\mathrm{c}\right)}. \tag{16}$$

The maximum amplification efficiency for a train of short pulses is achieved for energy density

$$Q_\mathrm{opt} = Q_\mathrm{s}\ln\left\{2\exp\left(-\frac{\Delta t}{\tau_\mathrm{c}}\right)+\frac{g_0}{\alpha_{ns}}\left[1-\exp\left(-\frac{\Delta t}{\tau_\mathrm{c}}\right)\right]^2\right\}$$

and is

$$\eta_\mathrm{ext} = \frac{1}{\Delta t/\tau_\mathrm{c}}\left\{\frac{\left[1-\exp\left(-\Delta t/\tau_\mathrm{c}\right)\right]\left[1-\exp\left(-\varepsilon\right)\right]}{1-\exp\left(-\varepsilon\right)\exp\left(-\Delta t/\tau_\mathrm{c}\right)} - \frac{\alpha_{ns}\varepsilon}{g_0}\right\}. \tag{17}$$

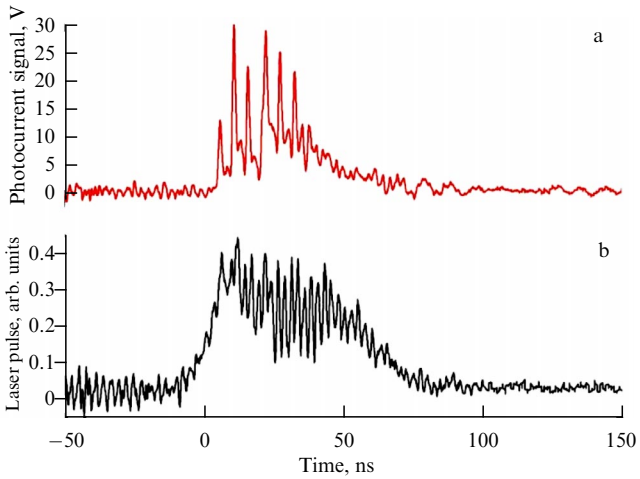


**Figure 8.** Oscillograms of amplitude-modulated laser pulses (b) and photocurrent in the ionized air gap (a) during injection of a USP train into the resonator. The USP amplitudes in the oscillograms are underestimated by a factor of 1000 due to the limited time resolution of the photodetector.

For a pulse repetition interval $\Delta t \approx \tau_\mathrm{c} = 2$ ns, for $Q_\mathrm{opt} = 3.1-4.3$ mJ cm$^{-2}$, we obtain $\eta_\mathrm{ext} = 0.38-0.48$. The amplification efficiency of a short pulse train with respect to pumping, $\eta_\mathrm{train} = \eta_\mathrm{ext}\eta_\mathrm{p} = 0.095-0.12$, in this case is comparable to the amplification efficiency of long pulses.

### 2.4 Simultaneous amplification of a train of short and long pulses

The rapid recovery of population inversion in the gain medium of a KrE laser makes it possible to simultaneously amplify both long and short pulses. While the amplification of single short pulses in a long double-pass amplifier occurs on a quasi-stationary profile of the gain $g(x)$ created by the ASE (see Fig. 7), the energy and efficiency of USP amplification will be noticeably lower than in the case considered above, $g(x) \equiv g_0$. A similar picture arises with the simultaneous quasi-continuous amplification of long pulses (or their train after the multiplexer) and short pulses [59], with the significant difference that in such a system there are no losses for the ASE and it is possible to combine the amplified long and short pulses on the target to ensure a complex temporary form of power input. Specifically, a promising LTS scheme with shock ignition [61] calls for pulses with a sharp, almost two orders of magnitude, increase in power during the last 100–200 ps. In addition, by suppressing ASE with long pulses, it is possible to significantly increase the contrast of short pulses by directing them into the amplifier at small angles to the long ones, which is of interest for producing a laser-plasma X-ray source used for transmission diagnostics of the target.

The hybrid Ti:sapphire–KrF GARPUN-MTW laser demonstrated regenerative amplification of subpicosecond USPs in a cavity where quasi-stationary lasing simultaneously developed [60]. As a result, combined pulses were obtained, consisting of long 100-ns pulses, which contained most of the energy, and USPs, which had a duration of $\sim 1$ ps and a peak power three orders of magnitude higher. On the oscillogram in Fig. 8a, their amplitude is underestimated by approximately 1000 times due to the limited time resolution of the photodetector ($\sim 1$ ns). Amplitude-modulated pulses combined efficient resonantly enhanced ionization of water

vapor in atmospheric air by powerful USPs and maintaining the electron density in the channel due to the suppression of attachment to oxygen by low-intensity 100-ns radiation from the pedestal (Fig. 8b). Such pulses have found application for initiating long electric discharges [62, 63] and producing plasma waveguides in atmospheric air for highly directional transport of microwave radiation [64] (for more details, see Section 3.2).

## 3. High-power excimer laser systems

### 3.1 Laser systems for generating single pulses

In this section, we review the most significant advances in the development of high-power, large-scale electron-beam pumped excimer lasers. Table 2 lists large excimer laser systems with a gain medium volume of 20 liters or more used as powerful pulse generators or amplifiers. The most impressive results have been obtained at a number of companies and national laboratories in the USA, where Maxwell Laboratory Inc. (MLI) launched the first large KrF laser with a chamber length of 2 m and a volume of 60 l as early as 1977 [43]. Subsequent improvement in the laser involved increasing the duration of the electron beam pump pulse and the generated radiation from 2 to 4 μs. For the same energy, a long pulse duration has some advantage in the propagation of radiation in the atmosphere due to the reduction in nonlinear effects and, in addition, reduces the requirements regarding the radiation resistance of optical elements. Long pumping is also necessary in generators to settle a narrow angular or spectral composition of radiation, as well as to implement mode locking [65].

The large-scale Scaleup excimer laser with a volume of 1000 l was launched by AVCO in 1981 [43]. It was the first to use a double-sided transverse pumping scheme with counter-propagating electron beams, which were introduced into the laser chamber perpendicular to its optical axis. This geometry makes it possible to uniformly pump a large volume of a gain medium, which was often subsequently used in other large-scale facilities. The problem of manufacturing large-sized optical windows for a laser chamber was also solved. This setup demonstrated the conversion of UV radiation with wavelength $\lambda = 351$ nm by stimulated Raman scattering (SRS) in compressed hydrogen with an efficiency of about 25%. A high quality laser beam with a divergence close to the diffraction-limited one was obtained in the blue-green region of the spectrum [66, 67].

The RAPIER B (Raman Amplifier Pumped by Intensified Excimer Radiation) facility was made at the Lawrence Livermore National Laboratory (LLNL) in 1981 [68]. Just like its previous smaller version, RAPIER A, it was intended for experiments on compression and summation of KrF laser pulses due to SRS, as an alternative to the angular pulse multiplexing scheme [56, 57]. The goal of these experiments was to shorten KrF laser pulses into the nanosecond range of durations required for LTF [69]. The setup served as a prototype for many other large KrF amplifiers developed for LTF. It used shorter ($\sim$ 150 ns) high-voltage accelerating voltage pulses in vacuum diodes, which were formed in a two-stage circuit with resonant recharging of a voltage pulse generator (VPG) to double forming lines (DFLs) with deionized water, as well as bilateral transverse pumping of the gain medium by two electron beams directed towards each other with stabilization in a magnetic field [70]. It was possible to demonstrate a width narrowing of the radiation spectrum to $\sim 7$ cm$^{-1}$, which was necessary for effective SRS conversion [69], and a decrease in the radiation divergence to $\sim 10^{-4}$ rad due to the injection of narrow-band radiation into an unstable laser cavity. Injection control of the spectral and angular characteristics of excimer lasers was studied in more detail in Ref. [71].

The largest excimer laser of all, made for the US Department of Defense, was the Super Large Aperture Module (SLAM), which was developed at Thermo-Electron Technologies Corp. (TTC) [43]. The facility was supposed to demonstrate 'Raman beam cleanup technology' — a method of SRS beam cleaning, i.e., the possibility of obtaining a high-quality beam after a Raman amplifier pumped by an excimer laser with high energy, but of lower radiation quality. In 1986, this laser produced a laser energy of 6.5 kJ at wavelength $\lambda = 308$ nm with an efficiency of 5.6% when pumping a working Xe/HCl/Ar mixture at a pressure of 1.5 atm. Somewhat later, SLAM generated energy up to 8 kJ with XeCl and 15–20 kJ with KrF in pulses 650 ns in duration. Since then, according to the original design, the quality of the optics of the setup could be not too high, four independent unstable resonators were mounted in the $100 \times 100$-cm laser aperture, and the quartz output windows consisted of 16 separate elements. This solution significantly reduced the cost of optical elements, the cost of which was extremely high for a similar excimer module, LAM, at the Los Alamos National Laboratory (LANL). Unlike AVCO, the Raman amplifiers were pumped by four UV laser beams directed at an angle to the amplified Stokes radiation. The UV radiation linewidth of 0.012 cm$^{-1}$ required for efficient conversion in compressed hydrogen was provided by independent injection into the resonators of narrow-band radiation from the master oscillator, previously amplified in the XeCl amplifier. A frequency-doubling dye laser was used as the master oscillator. At the output of the Raman amplifier, radiation was obtained at wavelength $\lambda = 353$ nm with a diffraction divergence and an energy of over 1 kJ. The conversion efficiency was 70%. In addition, the capabilities of 'Raman look-through operation' were demonstrated — a method for correcting phase distortions induced in the atmosphere by amplifying in the Raman amplifier a probing low-energy laser beam with a reversed wavefront.

The KrF Large Aperture Module (LAM) laser module, which was developed jointly by TTC and LANL, was a modification of SLAM and was used as a two-pass final amplifier of the Aurora multistage setup intended for research on LTF [44, 45]. In the free-run oscillation mode with a non-optimal unstable resonator, it yielded an energy of 10 kJ with an efficiency of 6.5%, and 5–6 kJ in the two-pass amplifier mode [72]. It is claimed that, on optimization, the LAM could provide an output energy of 15–20 kJ in amplification mode. The LAM $F_2$/Kr/Ar working mixture with a pressure of 600–1200 Torr was pumped by two counterpropagating electron beams with an energy of 675 keV and a current density of 12 A cm$^{-2}$. A square exit window of the laser cell with dimensions of $100 \times 100$ cm was made of a 7-cm-thick quartz plate.

The multi-stage KrF laser Aurora facility consisted of a master oscillator, an optical system for spatial and temporal beam separation — an angular multiplexer, three preamplification stages, a final stage, and a demultiplexer — a system for simultaneous convergence of beams on the target. Angular multiplexing, which was the basis for the construc-

**Table 2.** High-power pulsed excimer lasers with electron beam pumping.

| Laboratory, laser | Chamber dimensions or volume | Gain medium | Radiation wavelength, nm | Energy, J/pulse | Pulse duration, ns |
|---|---|---|---|---|---|
| **USA** | | | | | |
| Maxwell Lab. Inc. [43] | $L = 200$ cm; $V = 60$ l | KrF | 248 | 300 | 2000 – 4000 |
| AVCO Research Lab., Scaleup [43] | $V = 1000$ l | XeCl<br>XeF<br>KrF | 308<br>353<br>248 | 4000<br>5000<br>5500 | 2000<br>2000<br>2000 |
| Thermo-Electron Technologies Corp., SLAM [43] | $100 \times 100 \times 200$ cm; $V = 2000$ l | XeCl | 308 | 6500 | 650 |
| Livermore National Lab., RAPIER B [43] | $30 \times 30 \times 150$ cm; $V = 130$ l | KrF | 248 | 850 | 150 |
| Los Alamos National Lab., LAM Aurora [60] | $100 \times 100 \times 200$ cm; $V = 2000$ l | KrF | 248 | 10,000 | 650 |
| Naval Research Laboratory, Nike [67] | $60 \times 60 \times 200$ cm; $V = 720$ l | KrF | 248 | 5000 | 240 |
| **Great Britain** | | | | | |
| Rutherford Appl. Lab., Sprite [121];<br>Titania [130] | $\varnothing$ 27 cm, $L = 100$ cm; $V = 60$ l<br>$\varnothing$ 42 cm, $L = 150$ cm; $V = 200$ l | KrF<br>KrF | 248<br>248 | 150<br>1000 | 60<br>170 |
| **Japan** | | | | | |
| Institute for Laser Science of University of Electro-Communications [153] | $\varnothing$ 28 cm, $L = 100$ cm; $V = 60$ l | KrF | 248 | 460 | 100 |
| Electrotechnical Lab., ASHURA [143];<br>Super-ASHURA [147] | $\varnothing$ 29 cm, $L = 100$ cm; $V = 66$ l<br>$\varnothing$ 60 cm, $L = 200$ cm; $V = 570$ l | KrF<br>KrF | 248 | 700<br>2700 | 100<br>270 |
| Institute for Solid State Physics of Tokyo University [157] | $23 \times 23 \times 80$ cm; $V = 42$ l | KrF | 248 | 160 | 70 |
| **China** | | | | | |
| China Institute of Atomic Energy, Heaven-I [158] | $\varnothing$ 27 cm, $L = 100$ cm; $V = 57$ l | KrF | 248 | 400 | 200 |
| Northwest Institute of Nuclear Technology [162] | $\varnothing$ 38 cm, $L = 100$ cm; $V = 110$ l | XeCl | 308 | 500 | 200 |
| **USSR and Russia** | | | | | |
| Kurchatov Institute of Atomic Energy [198] | $V = 20$ l | XeCl | 308 | 100 | 1000 |
| Institute of High Current Electronics [200];<br>[201];<br><br>[202] | $\varnothing$ 20 cm, $L = 150$ cm; $V = 45$ l<br>$\varnothing$ 20 cm, $L = 100$ cm; $V = 30$ l<br>$\varnothing$ 60 cm, $L = 200$ cm; $V = 600$ l | XeCl<br>XeCl<br>KrF<br>XeCl | 308<br>308<br>248<br>308 | 150<br>110<br>90<br>1900 | 220<br>300<br><br>250 |
| Lebedev Physical Institute, RAS, GARPUN [173] | $14 \times 18 \times 100$ cm; $V = 25$ l | KrF | 248 | 100 | 100 |

tion of the entire system, made it possible to divide the initial 5-ns pulse required for LTF into 96 beams using beam splitters. Matching the amplifier pumping duration of 650 ns, the duty cycle and the total duration of the train ensured efficient extraction of stored energy from the amplifier. Of the 96 amplified beams, 48 were intended directly for interaction with targets, containing up to 1.5 kJ of energy with a variable pulse duration of 3–20 ns; the remaining beams were supposed to be used for various diagnostics. In plane geometry, when all beams were brought together into a single focusing spot with a diameter of 600 μm on the target, an intensity of up to $3 \times 10^{14}$ W cm$^{-2}$ was achieved. Solving the problem of synchronous operation of the master oscillator and amplifier stages, automatic alignment of an extremely complex optical system made it possible to carry out one to four full-scale facility launches per day. It was planned to achieve the following parameters: the energy delivered to the target in 48 beams was 5 kJ, the focusing spot

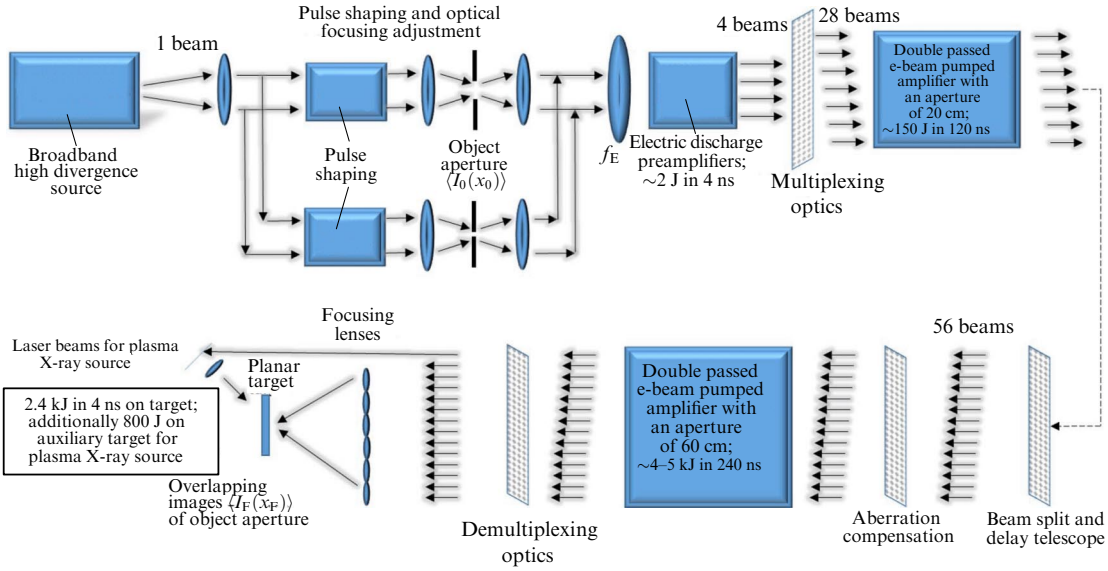


**Figure 9.** Optical diagram of the Nike KrF laser system at the US Naval Laboratory. (Reprinted with permission, © The Optical Society [81].)

was 300 μm, and the radiation intensity was $10^{15}$ W cm$^{-2}$. Although these parameters were never implemented due to the cessation of the research program, the experience of operating the Aurora facility and the first results obtained with it served as the basis for a new design of a full-scale installation for LTF with an energy of about 5 MJ and a pulse duration of 10 ns [73]. Power Amplifier Modules (PAMs), designed for an output energy of 100 kJ, were developed for the final amplifier stages of this facility [46, 47]. The possibilities of scaling KrF laser modules for LTF were also discussed in Ref. [74], and various schemes for constructing thermonuclear power plants (fusion reactors) with KrF-laser drivers were first considered in Refs [75, 76].

The shortcomings revealed in the operation of the Aurora facility [77], in particular, the too long pumping time of the amplifiers and the associated complex and expensive optical pulse multiplexing system, were taken into account when developing the 56-beam multi-stage KrF Nike laser facility at the Naval Research Laboratory (NRL), which was developed as part of the Inertial Fusion Energy (IFE) program of the US Department of Energy. This new-generation facility, launched in 1995 [78], was the first to use the principle of induced spatial incoherence of laser beams, which makes it possible to eliminate the microscale speckle structure in the focal spot characteristic of coherent radiation [79, 80]. Nike's optical configuration is schematized in Fig. 9 [81]. From the radiation of a broadband incoherent discharge-pumped KrF source, which differed from a conventional laser in the absence of an output cavity mirror, i.e., actually generating incoherent ASE, four pulses with the required duration of $\sim 4$ ns and angular distribution [82] were formed using electro-optical gates and aperture stops, which were then amplified to an energy of $\sim 2$ J in discharge-pumped amplifiers with X-ray preionization [83]. At the next stage, after angular multiplexing, 28 beams were amplified in two passes through a preamplifier with gain region dimensions of $20 \times 20 \times 100$ cm and electron beam pumping with a duration of 120 ns. Finally, after doubling the number of beams, a train of 56 pulses was amplified in two passes in the final amplifier with dimensions of $60 \times 60 \times 200$ cm and an electron beam pump duration of 240 ns. The radiation energy at the system output amounted to 4–5 kJ. After the demultiplexer, 44 pulses of incoherent radiation with a total energy of up to 3 kJ simultaneously arrived at a plane target. As a result, the inhomogeneity of target irradiation was $\leqslant 0.2\%$ [84, 85], which is the smallest value ever obtained in laser experiments. The remaining 12 beams with an energy of $\sim 800$ J were used to generate a laser-plasma X-ray source to diagnose the laser–target interaction.

The current status of the pulsed Nike laser system and the repetition-rate Electra laser made in the same laboratory, analysis of various limiting physical and technological factors, predictions for the improvement of facility parameters, as well as the principles of developing a KrF laser driver with megajoule energy are considered in comprehensive review Ref. [81]. Simultaneously with laser experiments at NRL, intensive studies were carried out on hydrodynamic instabilities during the acceleration of thin flat slabs of materials [86–93]. These experiments confirmed the ideas about the advantages of UV laser radiation for interaction with plasma (see, for example, reviews [94, 95]), namely: (1) short-wave radiation penetrates deeper into the plasma, since its critical density $n_{cr} \propto \lambda^{-2}$ is higher, and it is absorbed more efficiently in denser plasma to produce a higher ablation pressure $p$; (2) for UV radiation in the plasma corona with a density below the critical one, the thresholds for the development of plasma instabilities are higher, whose value $\propto I\lambda^2/p$ is determined by the ratio of the ponderomotive radiation pressure to the pressure in the plasma; (3) a higher ablation rate of the accelerated target shell prevents the development of Rayleigh–Taylor hydrodynamic instability at the boundary with the plasma. Additional advantages for stable compression of a spherical thin-walled capsule with thermonuclear deuterium–tritium (DT) fuel in the LTF scheme with direct laser irradiation (direct-drive ICF) are provided by the large width of the KrF laser radiation spectrum ($\sim 3$ THz) and high uniformity of irradiation with incoherent radiation. Experiments have demonstrated a gradual decrease in the size of the irradiation spot on the target as it is compressed (optical zooming) [79, 96], which eliminates the redistribution of energy between many beams during their nonlinear interaction with the plasma corona (crossed-beam energy transfer) [97], increasing the efficiency of target heating and the symmetry of its irradiation.

As a result of experimental research and theoretical simulations, and analysis of various concepts for obtaining energy through LTF (IFE) [94, 95, 98–104], two prototypes of energy facilities with a KrF laser driver, Fusion Test Facilities (FTFs), were proposed [102, 104]. Using these facilities, it would be possible to check the correctness of the adopted concepts, test various elements of a future thermonuclear reactor, and check their reliability at high doses of irradiation by the DT reaction products: neutrons, X-ray and gamma radiation, multiply charged ions. In the latest FTF version [104], a multilayer spherical target is irradiated with profiled laser pulses from a KrF laser with a sharp increase, by 1–2 orders of magnitude, in power during the last $\sim 250$ ps for a total pulse duration of $\sim 10-15$ ns. This regime, first proposed by V A Shcherbakov [106] and subsequently called 'shock-ignition ICF' [61], allows us to separate the stages of compression of relatively cold DT fuel to a high density and its subsequent ignition by a powerful shock wave converging towards the center of the target, initiated by the high-intensity final part of the laser pulse. Two-dimensional simulations for the optimal DT target [105] showed that an energy of 500 kJ in profiled pulses is capable of providing gain factor (the ratio of the released thermonuclear energy to the laser energy) $G_T \geqslant 130$. With the full efficiency of the KrF laser driver (the ratio of the radiation energy to the initially stored electrical energy) $\eta_D = 7\%$, this is enough to satisfy condition $G_T\eta_D \geqslant 10$, which is necessary to make a closed-cycle power plant operating with a pulse repetition rate of 5–10 Hz and providing reproduction of energy expenditure for pumping the driver (see, for example, Ref. [107]). The driver was to use 35 final KrF amplifiers with dimensions of $60 \times 100 \times 200$ cm and an output energy of 17 kJ, extracted in an angular multiplexing configuration with a train of pre-shaped pulses [108].

Such a KrF laser system could be the link between the demonstration of ignition of the DT fusion reaction at the world's largest neodymium laser system, the National Ignition Facility (NIF) at the US Livermore National Laboratory (LLNL) with megajoule energy at the third harmonic ($\lambda = 353$ nm) in single pulses [109, 110], and a future power plant of repetition-rate operation based on LTF. The NIF facility uses a scheme of so-called indirect compression of shell targets (indirect-drive ICF) with secondary X-ray radiation [107], which makes it possible to improve the uniformity of irradiation of spherical capsules with DT fuel placed in a cylindrical converter (hohlraum). Although in this case it has not yet been possible to fully overcome the hydrodynamic instabilities that prevent the achievement of the design compression of the DT fuel and lead to its mixing with the shell material, in recent experiments on December 5, 2022, a thermonuclear neutron yield of $\sim 10^{18}$ per pulse was obtained. For the first time in laser experiments, thermonuclear fuel was ignited and heated by $\alpha$ particles, and the released energy of 3.15 MJ exceeded the laser energy of 2.05 MJ, i.e., $G_T > 1$ was achieved. This was stated in a press release from LLNL and the US Department of Energy on December 13, 2022 [111].

This result of paramount significance and the ongoing construction of other megajoule solid-state laser systems, such as LMJ in France [112], UF2-ML (the original name of this project was Iskra-6) in Russia [113, 114], and Shenguang in China [115–117], inspire optimism in the practical implementation of a laser thermonuclear reactor with $G_T\eta_D \geqslant 10$. An increase in $G_T$ can be expected with direct target compression due to a decrease in energy losses associated with the conversion of laser radiation into X-rays in a promising shock ignition scheme [61]. All of the mentioned solid-state devices using optical pumping with flash lamps have a very low total efficiency of $\sim 0.1\%$ and operate in single pulses with an interval of several hours. Laser drivers of energy thermonuclear installations (IFE) must have megajoule energy with a pulse repetition rate of 5–10 Hz and a long-term resource of non-stop operation for at least one year. The development of such drivers invites completely different approaches, for example, laser crystals or ceramics as the gain medium, cooled by a fast gas flow or liquid nitrogen, with narrow-bandwidth pumping by semiconductor light-emitting diodes. This technology, called a diode-pumped solid-state laser (DPSSL), was first demonstrated at the Mercury facility (LLNL) [118]. The laser generated nanosecond radiation pulses with wavelength $\lambda = 1051$ nm and an energy of over 50 J at a repetition rate of 10 Hz and a total efficiency of 5%. The resource of non-stop operation of the facility was 300,000 pulses in several series lasting 0.5–2 hours. Scaling the DPSSL technology to thermonuclear facilities at a megajoule energy level is a very intricate task. Some conceptual approaches to solving it were considered in the pan-European High Power Laser Energy Research Facility (HiPER) project within the framework of the European Strategy Forum on Research Infrastructures (ESFRI) program [119].

Among other potential LTS reactor drivers, a KrF laser with the unique properties listed above best meets the basic physical, technological, and economic requirements for power plants based on LTF. Demonstrated at NRL, at the Electra facility (Fig. 10), was the long-term operation of a KrF laser with an energy of 700 J in a repetition-rate mode at 5 Hz (50,000 pulses in a continuous train or 300,000 in total over 8 days) [81]. The ArF laser is also of great interest, with which, back in the 1970–1980s, a free-run lasing energy of about 100 J and a physical efficiency of $\sim 3\%$ were obtained under pumping by an electron beam with a duration of 50–65 ns [22, 120]. Using the Electra setup converted to operate with an ArF laser in the free-running mode under non-optimal excitation conditions from a limited volume (the optical cavity mirrors did not cover the entire laser aperture), an energy of $\sim 140$ J was obtained [121]. When

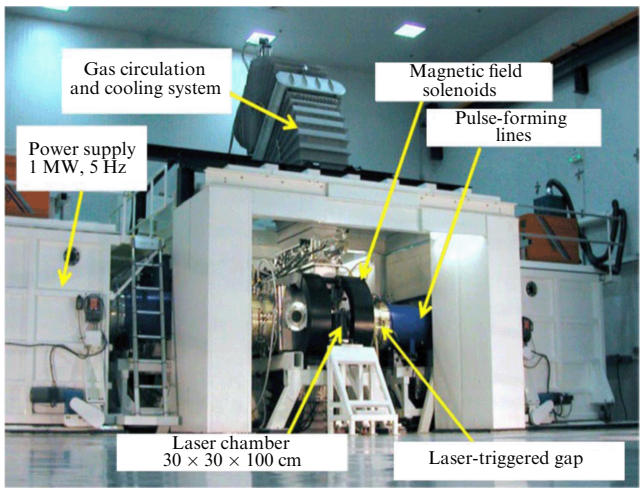


**Figure 10.** Repetition-rate KrF Electra laser at the US Naval Laboratory. (Reprinted with permission, © The Optical Society [81].)

operating this laser as a two-pass amplifier, an efficiency of $\sim 16\%$ is predicted, which, along with a wide gain bandwidth of $\sim 10$ THz and the shortest wavelength of 193 nm among all existing noble gas halide lasers, makes the ArF laser an attractive driver for a future LTF reactor [122, 123].

Among European laser centers, the greatest achievements in the development of large excimer lasers belong to the Rutherford Appleton Laboratory (RAL) in the UK, where the Sprite multi-stage KrF laser system was made for a wide range of tasks related to plasma heating, research on X-ray lasers on multiply charged ions, and LTF [124]. The main amplifier of this system had an original configuration with a four-sided injection of electron beams into a 100-cm-long cylindrical cell 27 cm in diameter, which made it possible to uniformly excite a gain volume of 58 l without using a magnetic field, putting about 3 kJ of energy into it in 60 ns. In oscillator mode, when narrow-band radiation with an energy of 50 mJ was injected into an unstable telescopic resonator with magnification $M = 4$, Sprite produced output radiation pulses with an energy of about 150 J, a duration of 60 ns, a divergence of 70 μrad, and a narrow linewidth of $0.3\ \text{cm}^{-1}$, which was required for effective nonlinear radiation conversion by SRS.

The Sprite laser system was one of the first excimer lasers to be used to amplify ultrashort picosecond pulses [125]. This system consisted of a picosecond front-end based on a dye laser with frequency conversion to the third harmonic, an EMG 103 MSC (Lambda Physik) discharge-pumped amplifier, and two amplifiers with electron beam pumping, Goblin (aperture: 6 cm; length: 40 cm) and Sprite, each of which amplified the pulses in a two-pass configuration. Since the energy density at the output of the KrF amplifier for pico- and subpicosecond pulses cannot exceed 20–40 mJ $\text{cm}^{-2}$ in the saturation mode (see Section 2.2), the output USP energy was limited by the size of the output aperture. At the output of the Sprite wide-aperture amplifier, ultrashort pulses with a record energy of 2.5 J and a duration of 3.5 ps were obtained, which corresponded to a peak output power of 0.7 TW. This was 230 times higher than the nominal power of laser pulses when operating in oscillator mode. When focusing radiation onto a spot with a diameter of 25 μm, the intensity on the target amounted to $5 \times 10^{15}\ \text{W cm}^{-2}$, although the contrast, i.e., the ratio of USP energy to ASE energy along the amplifier axis, was low due to the lack of optical isolation (saturable absorbers) between the amplifier stages.

An effective method was developed at RAL for producing picosecond radiation pulses with a high contrast and a low divergence, which involved a combination of angular multiplexing and summation of many beams in cells with an SRS-active gas [126, 127]. A train of picosecond ultrashort pulses formed by the multiplexer, spaced from each other by several nanoseconds, which is the recovery time of the population inversion in the KrF-gain medium, was divided into several beams, which were amplified in cascades of KrF amplifiers and then pumped the Raman oscillator and Raman amplifiers. Since the gain during SRS conversion depends exponentially on the pump power, the pulse contrast in such a system can be very high. Experiments performed with $H_2$, $CH_4$, $SF_6$, and $NH_3$ demonstrated a high efficiency of pump radiation conversion into the first Stokes component, which ranged up to 70% for forward scattering.

Angular multiplexing and SRS summation [127, 128] were the basis for the design of a more powerful Super Sprite laser system [129–131]. It was assumed that this system would have an output energy of up to 7 kJ with a pulse duration varying from 3 ps to 3 ns and a maximum power of up to 750 TW with a diffraction divergence of the converted radiation at wavelength $\lambda = 268-277$ nm. In addition to the Goblin and Sprite amplifiers, it was planned to manufacture two more amplifier stages. The new Titania amplifier, which was put into operation, had a cylindrical cell with an aperture of 42 cm and a length of 150 cm. It was pumped from four sides by electron beams with a pulse duration of 170 ns and was designed for an output radiation energy of 1.0 kJ in the free-running mode. Another amplifier, Oberon, with a sectioned aperture of 150 cm and a cell length of 350 cm, was designed for an output energy of 15 kJ when pumped by 12 electron beams from six sides. With the Super Sprite KrF laser system with the new Titania final amplifier, in a subpicosecond pulse, a peak power of up to 10 TW and a radiation intensity on the target of $10^{20}\ \text{W cm}^{-2}$ were expected, which would allow research to justify another promising LTF scheme with fast-ignition ICF [132–134].

In the fast ignition approach, as well as in the shock ignition approach, the stages of DT fuel compression by nanosecond pulses and subsequent ignition are separated in time, the ignition being carried out by fast electrons with an energy of $\sim 1$ MeV that penetrate into the compressed fuel [135]. Fast electrons are generated in a rarefied plasma corona by a powerful 20-ps pulse due to the development of plasma instabilities. To effectively transport them to the dense core, use is made of a second pulse with a duration of $\sim 100$ ps, which produces a 'channel' in the dense plasma due to the ponderomotive radiation pressure. Reviews [136, 137] also considered other methods of fast ignition using accelerated protons or heavy ions, which make it possible to reduce the energy of the main nanosecond laser driver.

Short-wavelength KrF laser radiation can be focused onto a small spot $S \propto \lambda^2$ in size, and hence a higher intensity can be obtained at the target $I \propto P\lambda^{-2}$ for a given peak pulse power $P$. In turn, the values of the ponderomotive pressure responsible for the passage of radiation through the plasma corona and the energy transferred to fast electrons are both determined by the parameter $I\lambda^2 \propto P$, i.e., are independent of the wavelength. The advantage of UV radiation for the LTF procedure under consideration is that, penetrating into a denser plasma with a critical density $n_{\text{cr}} \propto \lambda^{-2}$, it transfers energy to a larger number of accelerated electrons and thereby heats the compressed DT fuel more efficiently.

In the direct amplification of short spectrally limited pulses in KrF laser systems, the nonlinear interaction of ultrashort supercritical pulses with amplifiers and other pass-through elements of the optical path limits the maximum achievable radiation power [138, 139], although not as strongly as in solid-state lasers. Nonlinear processes are also significant during the propagation of high-power UV pulses along an extended air path between amplification stages in an angular multiplexer and demultiplexer [139, 140]. Two methods of amplifying high-power ultrashort pulses were experimentally tested on the Super Sprite laser system. In both cases, a Ti:sapphire front-end was used as a master USP oscillator, whose radiation was converted into the third harmonic coinciding with the amplification band of the KrF gain medium. In the former case, a chirped pulse amplification scheme was used [141]: the initial ultrashort pulses with a duration of 150 fs and an energy of $\sim 0.5$ mJ were stretched in time to $\sim 50$ ps using an optical stretcher and modulated in

frequency, after which they were amplified in wide-aperture Sprite amplifiers and Titania up to an energy of 7 J [132]. However, during subsequent compression of the pulses in an optical compressor, it was necessary to attenuate the energy to avoid destruction of the diffraction gratings. As a result, the USP energy after the compressor did not exceed 0.25 J with a duration of 750 fs, and the achieved radiation intensity of $10^{18}$ W cm$^{-2}$ in a focal spot of 1.5 μm was two orders of magnitude lower than planned. Although amplification of chirped ultrashort pulses in principle solves these problems in KrF systems [142, 143], the low radiation resistance of diffraction gratings in the UV range, their high cost for laser beams with a large cross section, as well as the large number of laser beams in the angular multiplexing mode make it markedly difficult to implement this method in practice. An alternative approach was to use a train of spectrum-limited narrowband pulses with a duration of 10–60 ps to pump a Raman oscillator and Raman amplifiers with methane as radiation summator [133]. It was expected that the total energy in a train of 60-ps pulses after KrF amplifiers in the angular multiplexing scheme in the Super Sprite system would be $\sim$ 130 J, and after SRS summation with an efficiency of 70%, the energy in one 60-ps pulse at a Stokes wavelength of 268 nm will be $\sim$ 100 J. However, these plans were not implemented, since work with the KrF laser was terminated, and further experiments at RAL on amplification of chirped ultrashort pulses were carried out on the Vulcan petawatt-class solid-state laser system.

Japanese research in the field of high-power excimer lasers is represented in Table 2 by three scientific centers. The largest facility, Advanced System for High-Power UV Radiation Application (ASHURA), was made in the Electrotechnical Laboratory, later renamed the Advanced Institute of Science and Technology (AIST). The work in this laboratory, with minor differences, repeated the RAL program in the UK. The ASHURA laser consisted of a discharge-pumped master oscillator with a narrow emission line, a discharge-pumped amplifier, and two KrF amplifiers, Amp 2 and Amp 3, with electron beam pumping, as well as a system for Raman compression of laser pulses [144, 145]. The second amplifier, Amp 2, with a gain volume of $20 \times 20 \times 60$ cm, was transversely pumped by two electron beams and generated pulses with an energy of 230 J and a duration of 100 ns. The final 100-cm-long amplifier, Amp 3, with a cylindrical cell with a diameter of 29 cm, was excited symmetrically from four sides by eight electron beams with a pulse duration of 100 ns. In the free-running oscillation mode, the radiation energy from a gain volume of 66 l was 700 J, and, in the angular multiplexing scheme with double-pass amplification of six pulses with a duration of 15 ns, it was 660 J. The high specific pump power of up to 1.9 MW cm$^{-3}$ made it possible to work on mixtures with high Kr content. For such mixtures at a relatively low operating pressure of $\sim$ 1 atm, the physical efficiency can exceed 10%, and the saturation intensity, $\sim$ 10 MW cm$^{-2}$; as a result, they are promising for use in large-scale KrF amplifiers [146].

In the direct amplification of short pulses with a duration of 6 ps in a discharge-pumped amplifier and Amp 2, an energy of about 2 J was obtained at the ASHURA facility [147]. The master oscillator in these experiments was a dye laser with frequency conversion into the amplification band of KrF amplifiers. Developed for a larger-scale Super-ASHURA facility was a new final amplifier, Amp 4, which had a diameter of 60 cm and a length of 200 cm. Pumping from eight sides was carried out by 16 electron beams with a pulse duration of 270 ns. The specific pump power was lowered to 0.5 MW cm$^{-3}$, making it possible to maintain an acceptable level of ASE [148–150]. With double-pass amplification of 12 pulses with a duration of 20 ns in an angular multiplexing scheme and filling the amplifier aperture by 74%, a radiation energy of 2.7 kJ was obtained. To reduce the pulse duration to several nanoseconds, use was made of a cell with methane in which the efficiency of converting the radiation energy into the first Stokes component (wavelength $\lambda = 268$ nm) in the forward SRS scattering was as high as 73% [151]. With SRS backscattering, it was possible to reduce the pulse duration to 150 ps with a conversion efficiency of 27% [152]. At the same time, the peak radiation power increased by a factor of 30.

The KrF laser at the Institute for Laser Science (ILS) of the Tokyo University of Electro-Communications had a traditional transverse double-sided pumping scheme with electron beam stabilization by a magnetic field. With an energy input of 4.2 kJ, from a gain volume of 60 l (cell diameter: 28 cm; length: 100 cm), an output energy of 460 J was obtained in a 100-ns-long pulse [153]. Experimental studies and numerical simulations carried out at the facility made it possible to develop scaling criteria for KrF drivers for LTF. The maximum dimensions of the amplifier limited by the ASE were $3 \times 2 \times 10$ m [154]. With a very low pump power of 0.1 MW cm$^{-3}$, such an amplifier was capable of providing an energy of 500 kJ with an intrinsic efficiency of about 10%.

To shorten pulses from several ten nanoseconds to tens of picoseconds, a multistage SRS-oscillator-amplifier circuit was developed at ILS based on backward non-stationary Raman scattering of KrF laser radiation in methane, which made it possible to increase the peak power of the Stokes radiation at wavelength $\lambda = 268$ nm by a factor of 150 with a conversion efficiency of 22% [155]. In another setup, 10-ps seed pulses from an FL-4000 T master oscillator (Lambda Physik) based on an excimer-pumped dye laser with frequency doubling were sequentially amplified in discharge-pumped and wide-aperture KrF electron-beam amplifiers. To shorten the pulse duration and improve the contrast ratio, advantage was taken of saturable absorbers based on a solution of acridine in methanol [156]. At the output of the system, ultrashort pulses with an energy of 1 J and a half-maximum duration of 350 fs were obtained, which corresponded to a peak radiation power of 2.5 TW.

Research at the Institute for Solid State Physics at the University of Tokyo was also aimed at developing a pulsed subpicosecond terawatt-level KrF laser system [157]. The system operated in a generator–amplifier configuration and consisted of a subpicosecond ultrashort pulse oscillator based on a dye laser with radiation conversion into the third harmonic, a discharge-pumped KrF amplifier with gain region dimensions of $7 \times 7 \times 80$ cm, and a wide-aperture amplifier with electron beam pumping with dimensions of $23 \times 23 \times 80$ cm. The energy of free-run oscillation of the latter with an energy input of 1.8 kJ in 70 ns and a specific pump power of 0.6 MW cm$^{-3}$ was 160 J. With double-pass amplification of ultrashort pulses, an energy of 1.5 J was obtained at the output of the laser system in 390-fs-long pulses, which corresponded to a peak radiation power of 4 TW. In this case, the fraction of amplified spontaneous emission did not exceed 1.8%.

Later than other countries, China became involved in the creation of large excimer laser facilities intended for LTF, laser plasma research, and the equation of state of matter at

high pressures. One of them, the Heaven-I multifunctional KrF laser system, was constructed at the China Institute of Atomic Energy (CIAE) [158]. In the nanosecond version of this system, an LPX-150 discharge-pumped laser (Lambda Physik) with an energy of 400 mJ in 23-ns pulses was used as a master oscillator. Injection control of the angular radiation divergence in the oscillator and a spatial filter at the output served to improve the divergence of the initial radiation, which was sequentially amplified in two passes through a 50-cm-long preamplifier with a diameter of 12 cm, then through a final 100-cm-long amplifier with a diameter of 27 cm. In free-running lasing mode with an optimal resonator under bilateral transverse pumping by counterpropagating electron beams with a specific power of $\sim 1$ MW cm$^{-3}$, the latter yielded an energy of 400 J with a pulse duration of 200 ns. The facility uses an angular multiplexing technique with six beams, in which a total radiation energy of 120 J is obtained [159]. When focusing on a target onto a spot with a diameter of 220 μm, the radiation intensity was $\sim 10^{13}$ W cm$^{-2}$. To shorten the pulse duration to 5 ns and improve the beam quality, a scheme for converting KrF radiation in a Raman oscillator and three stages of methane Raman amplifiers was developed. It was expected that, with forward scattering, about 60% of the pump energy could be converted into Stokes radiation, which would produce an intensity at the target of $10^{14}$ W cm$^{-2}$ with spatial overlap of the three focused beams. In subsequent experiments [160, 161], the facility setup was modified to obtain a uniform intensity distribution when irradiating plane targets by introducing induced incoherence, similar to what was done with the Nike KrF laser. To do this, the output cavity mirror was removed from the LPX-150 master oscillator, and the incoherent ASE was retransmitted along the amplification path. The total energy of six pulses after amplification was 160 J with a duration of 25 ns. The inhomogeneity of the intensity distribution in the 400-μm focal spot was less than 1.6% at an intensity of $3.7 \times 10^{12}$ W cm$^{-2}$.

In experiments with short UV pulses, a Ti:sapphire Tsunami (Spectra Physics) front-end was used, which, after converting the radiation to the third harmonic, generated UV-USPs with a duration of 130 fs and an energy of $\sim 1$ mJ. The pulses were amplified in a two-pass off-axis configuration to an energy of 50 mJ in an LLG-50 discharge-pumped KrF amplifier (Laser Laboratorium, Gettingen) with an aperture of $4 \times 4$ cm, which operated at a repetition rate of 10 Hz. When focusing a USP with a duration of 440 fs on a target onto a spot with a diameter of 5 μm, the radiation intensity ranged up $10^{17}$ W cm$^{-2}$. With direct sequential amplification of USPs in a discharge-pumped KrF amplifier and wide-aperture amplifiers with electron beam pumping, the energy of a single USP (in one beam) after amplification was 2–3 J with a duration of 1.2 ps.

A high-power multistage XeCl laser system, made at the Northwest Institute of Nuclear Technology (NINT), was designed for uniform irradiation of plane targets due to the spatial overlap of 18 beams with induced spatial incoherence of the radiation [162, 163]. The incoherent radiation from a discharge-pumped XeCl oscillator was produced using a diffuse scatterer and then sequentially amplified in three discharge-pumped amplifiers. In the multiplexer, the pulses were distributed over 18 beams at small angles to each other, which were fed to the input of two wide-aperture amplifiers pumped by electron beams. The amplifiers were designed and manufactured at the Institute of High-Current Electronics (IHCE) of the Siberian Branch of the USSR Academy of Sciences in Tomsk. The smaller amplifier with a 25-cm aperture in free-running mode produced an energy of 90 J per pulse with a duration of $\sim 200$ ns. The large amplifier had an aperture of 38 cm and, when radially pumped from six sides, produced up to 500 J in free-running oscillation. When a train of 18 pulses with a half-maximum duration of 7 ns and a repetition interval of 10 ns was amplified, the total energy at the system output amounted to 80 J. After the demultiplexer, all pulses were simultaneously focused on the target onto a spot with a diameter of 860 μm with a radiation intensity of $\sim 10^{13}$ W cm$^{-2}$ and unevenness of 1.3%.

### 3.2 Work on high-power excimer lasers in our country

The first XeCl laser with a large gain medium volume of $20 \times 10 \times 200$ cm was launched at the Lebedev Physical Institute in 1981 [164]. When pumped by an electron beam with an electron energy of 200 keV, a current density of 4 A cm$^{-2}$, and a full-width at half-maximum pulse duration of 0.8 μs, an output energy of 4.8 J was obtained, and an output of 20 J was obtained in the electroionization version. Voltage was applied to the vacuum diode directly from the pulsed voltage generator (PVG), and the electron beam was injected into a laser cell on one side. At the Kurchatov Institute of Atomic Energy (IAE), with a similar method of one-sided transverse pumping but with a more effective matching of the PVG and the vacuum diode, it was possible to increase the current density to 40 A cm$^{-2}$ and obtain with XeCl an output energy of 100 J from a gain volume of about 20 l in a pulse approximately 1 μs long [165]. However, the distribution of pump energy and laser output was significantly nonuniform. The strong nonuniformity of excitation also limited the output parameters of the XeCl laser at the facility with a gain volume of 30 l made at the IHCE [166]. Pumping was carried out by an electron beam with an electron energy of $\sim 300$ keV, a current density of up to 15 A cm$^{-2}$, a pulse duration of $\sim 1.3$ μs, and an area of $150 \times 13$ cm. The transition to two-sided injection of electron beams into the laser chamber and an increase in the energy capacity of PVGs made it possible to significantly improve the uniformity of excitation and increase the gain volume of the laser to 45 l. For a current density of 20 A cm$^{-2}$, an output energy of 150 J per pulse with a full-width half-maximum duration of 220 ns and a divergence of 5 mrad was obtained [167].

A compact excimer laser with an output energy of 90 J with KrF and 110 J with XeCl in pulses with a duration of $\sim 300$ ns is described in Ref. [168]. It used a four-sided injection of radially converging electron beams into a laser chamber with a diameter of 20 cm and a length of 100 cm and a low-inductance PVG with vacuum insulation, located in the same volume with vacuum diodes. A similar arrangement of high-voltage power supplies (PVGs and pulse transformers) in a common vacuum volume together with diodes, which ensured low inductance and duration of electronic current pulses and reliable electrical insulation with compact dimensions, was also used in the above-mentioned wide-aperture XeCl amplifiers with energies of 90 and 500 J. These were made at IHCE for the excimer laser system at NINT in Xian (China) [162, 163]. The highest XeCl output laser energy of 1.9 kJ in 250-ns-long pulses was subsequently obtained in an IHCE using a similar scheme for generating accelerating voltage pulses under six-sided pumping of a gain volume of 600 l in a chamber with a diameter of 60 cm and a length of 200 cm [169].

The same principles of constructing electron accelerators were used in THL-30 wide-aperture photochemical amplifiers of femtosecond ultrashort pulses at the Lebedev Physical Institute [170] and THL-100 at IHCE [171], which operated at the XeF ($C \rightarrow A$) transition with wavelength $\lambda = 475$ nm in the photodissociation of $XeF_2$ molecules [39, 40]. The source of VUV radiation for photodissociation was the radiation of the $Xe_2$ dimer in the region of 172 nm, which arose when xenon compressed to 3 atm was excited by electron beams. Electron beams from several sides (four in THL-30 and six in THL-100) were introduced into a xenon converter located coaxially to the laser chamber. VUV radiation from the converter was injected into the chamber through windows made of calcium fluoride, which ensured uniform excitation of the gain medium in the amplifiers with apertures of $12 \times 12$ cm and 24 cm, respectively. At the output of the THL-100 were 30-fs-long pulses with an energy of 1.2 J and a peak power of 40 TW [172].

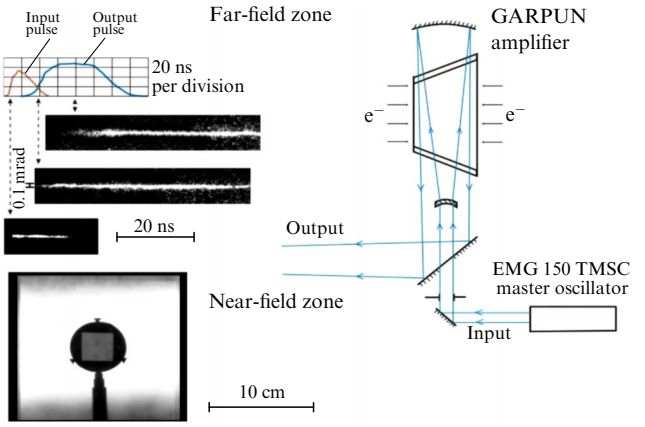


**Figure 11.** Optical configuration of the GARPUN laser in the mode of injection control and distribution of output radiation in the near- and far-field zones.

### 3.3 GARPUN KrF laser system at Lebedev Physical Institute

The KrF GARPUN (a transliteration from Russian for Gas Relativistic-Beam Pumped) laser was developed on the initiative of academician N G Basov and launched at the Lebedev Physical Institute in 1991 [173]. In fact, this was the first wide-aperture excimer laser in the country, which used a two-stage scheme of a pulsed high-voltage power supply of vacuum diodes with resonant recharging of PVGs on a DFL and transverse bilateral pumping of the gain medium with a volume of $16 \times 18 \times 100$ cm with electron beams stabilized by a magnetic field [174]. This arrangement ensured high uniformity of excitation of the $Ar/Kr/F_2$ working mixture with a specific pump power $W = 0.7-0.8$ MW cm$^{-3}$ and efficient generation of 100-ns pulses with an energy of 100 J and a peak power of 1 GW [175]. To control the angular and spectral composition of the radiation, 20 ns seeding pulses from a discharge-pumped KrF master oscillator were injected into the unstable laser cavity [176] (Fig. 11). In the injection control mode, the radiation divergence was 0.2 mrad, and the spectrum width was $\sim 0.2$ or $\sim 40$ cm$^{-1}$, depending on the spectrum of the master oscillator.

In 1996, a Berdysh preamplifier with a gain volume of $8 \times 8 \times 110$ cm [177] was added to the main KrF amplifier, with which using one-sided electron beam pumping and power density $W = 0.6-0.7$ MW cm$^{-3}$, an output energy of 25 J was obtained [178]. In a sequential two-pass amplification scheme of 20-ns master oscillator pulses, an output energy of up to 30 J with a peak power of 1.5 GW was achieved in both stages. Figure 12 shows photographs of the amplifiers as well as a general view of the GARPUN laser.


**Figure 12.** Photos of the GARPUN KrF laser: main amplifier (a), preamplifier (b), and general view of the facility (c).

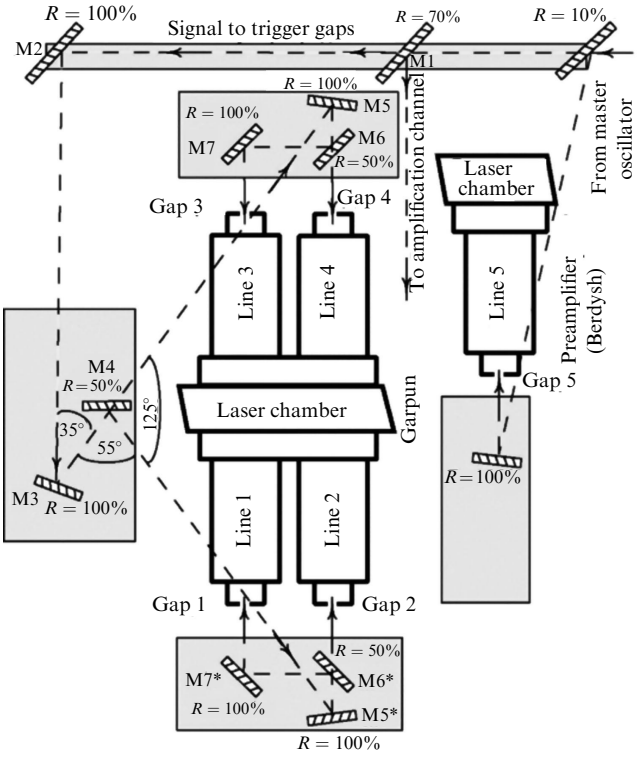


**Figure 13.** Synchronization of DFL in KrF amplifier stages with electron beam pumping and a KrF discharge-pumped master oscillator.

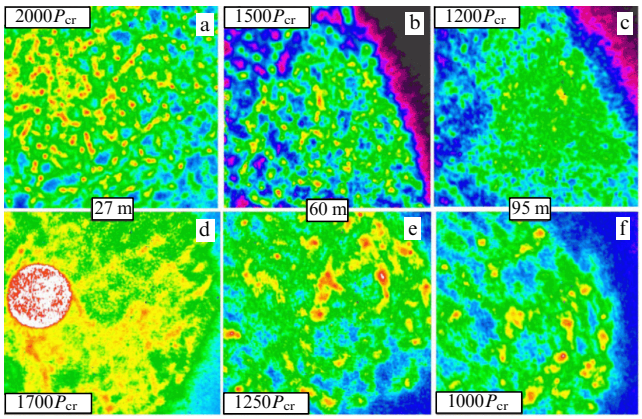


**Figure 14.** Distributions of radiation in a laser beam at various distances $L$ from the final amplifier: without (a–c) and with an Xe cell (d–f), placed at a distance of 5 m from the amplifier. Size of the imaged area is $4 \times 4$ cm. Peak USP power in units of $P_{cr} = 0.1$ GW is shown in the insets. Intensity in the images increases in the sequence of colors: violet, dark blue, blue, green, yellow, and red.

In 2006, the facility was equipped with a frequency-tripled Ti:sapphire Start-248 M front-end (Avesta Project LLC), which generated 100-fs pulses in the KrF amplification band [178]. Synchronization of the front-end and electron beam pumping of the amplifiers was carried out by a discharge-pumped KrF master oscillator, whose pulses ignited the gaps of five DFLs, which generated high-voltage pulses for the vacuum diodes of the preamplifier and amplifier (Fig. 13). The new hybrid Ti:sapphire–KrF laser system, called GARPUN-MTW, produced subpicosecond pulses with an energy of up to 0.6 J by direct amplification of ultrashort pulses [179]. Therefore, a terawatt power level was realized, which was comparable to that previously obtained using large KrF amplifiers with electron beam pumping.

Unlike the majority of previous studies, where nonlinear effects were not studied in detail (with the exception of Refs [180, 181]), in our experiments at the GARPUN-MTW facility it was possible to observe self-focusing and filamentation of the laser beam, which significantly affected the amplification of ultrashort pulses and their propagation along the 100 m of air route. Since the supercritical pulse power was four orders of magnitude higher than the critical power of self-focusing for UV radiation in air $P_{cr} = 3.77\lambda^2/8\pi n_0 n_2 \approx 0.1$ GW [182], where the linear refractive index is $n_0 \approx 1$ and the nonlinear index is $n_2 \approx 10^{-18}$ cm$^2$ W$^{-1}$, multiple self-focusing and the formation of optical filaments were observed during radiation propagation (Fig. 14). The laser beam decayed into several hundred filaments with a characteristic diameter $d_f = 240-340$ μm, whose intensity and energy density were several orders of magnitude higher than in background radiation [63, 64]. Coherent resonant two-photon excitation of the electronic state of water vapor $\tilde{C}\,^1B_1 \rightarrow \tilde{X}\,^1A_1$ and stimulated Raman scattering by rotational transitions of nitrogen were considered as possible filamentation mechanisms [183]. At a high intensity in the filaments $I_f = (2.0 \pm 0.6) \times 10^{11}$ W cm$^{-2}$, two-photon excitation led to effective three-photon $(2+1)$ vapor ionization (Resonance Enhanced MultiPhoton Ionization, REMPI), which proceeded through the intermediate $\tilde{C}\,^1B_1$ state with an anomalously large cross section $\sigma^{(3)} = (5.6 \pm 3.8) \times 10^{-27}$ cm$^6$ s$^{-1}$ W$^{-3}$ [184]. This produced weakly ionized continuous plasma channels in the atmospheric air with electron density $\rho_{ef} \approx 10^{13}$ cm$^{-3}$ [183]. Their continuous length ranged up to 15 m [185], and the filamentation region of the laser beam began 15 m from the output of the final amplifier and extended up to 60 m. The number of filaments in the beam cross section gradually decreased with distance $L$ due to the increasing nonlinear phase shift $\Delta = n_2 I_f L$ for high-intensity filaments compared to background radiation [186], which led to a loss of coherence of the laser beam. The maximum filamentation length was determined by the condition $\Delta \leqslant L_{coh}$, where coherence length $L_{coh} = \lambda^2/2\Delta\lambda$, and $\Delta\lambda = 2.5$ nm is the width of the emission spectrum broadened due to SRS.

Laser beam filamentation negatively affected the USP amplification. Developing in the air gaps between the amplifier stages and in the pass-through optical elements of the amplification path, including the windows of the amplifiers and spatial filter [187], it was responsible for additional losses during amplification. Optical elements made of calcium fluoride, although they have the lowest nonlinear absorption among all UV optical materials, they also exhibited nonlinear absorption and scattering of laser radiation, spectrum broadening beyond the amplification band of the KrF laser, as well as the formation of multiple microdefects along the filaments [188]. Furthermore, in the course of long-term operation, the transmission of the amplifier windows became lower due to photoelectronic excitation and the development of long-lived color centers under the influence of powerful UV radiation. Note that high-purity fused silica, commonly used in KrF amplifiers for nanosecond pulses, is completely unsuitable for high-intensity sub-picosecond pulses due to the high two-photon absorption.

Despite the fact that the filaments contained about 30% of the total energy of the laser beam, they were completely

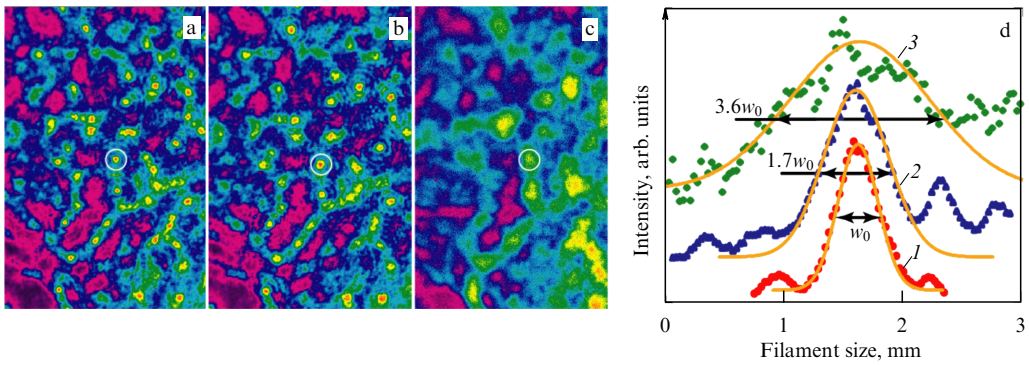


**Figure 15.** Same part of the cross section of a laser beam after passing through a cell with air (a), evacuated to $10^{-5}$ atm (b), filled with Xe at 0.1 atm (c) and the corresponding intensity profiles in filaments highlighted with a white circle (d) in air (*1*), a vacuum (*2*), and Xe (*3*). For clarity, curves are shifted along the vertical axis. Intensity in the images increases in the sequence of colors: violet, dark blue, blue, green, yellow, and red.

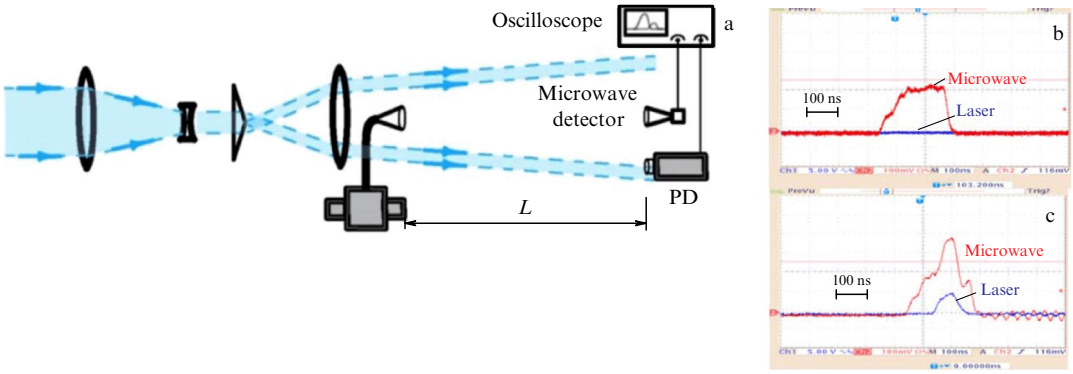


**Figure 16.** Experimental setup for the transmission of microwave radiation in a plasma waveguide (a), oscillograms of a laser pulse and a microwave signal on a detector located at distance $L = 60$ m from the emitter in the absence (b) and in the presence (c) of laser radiation.

absorbed in the gain medium of the KrF laser, since the energy density they transferred $Q_f = 0.2-0.06$ J cm$^{-2}$ was several times higher than the maximum energy density achievable by amplifying short pulses (see Section 2.3). As a result, premature saturation of the amplifiers was observed, the radiation energy density averaged over the beam being significantly lower than $Q_s$ [188], and the output beam was 'cleared' of the filaments. However, filamentation developed again ten meters from the output of the amplifiers.

To suppress beam filamentation, advantage was taken of a cell with xenon, which has a negative and large, in modulus, nonlinear refractive index at the wavelength of the KrF laser [189]. In the total nonlinear phase incursion, it compensated for the positive phase incursion in the amplifier windows, working gas, and air gaps between stages, when the so-called *B*-integral satisfied the condition

$$B = \frac{2\pi}{\lambda}\left(\int^{L_{Xe}} n_2^{Xe} I\,dl + \int^{L_{CaF_2}} n_2^{CaF_2} I\,dl + \int^{L_{wg}} n_2^{wg} I\,dl + \int^{L_{air}} n_2^{air} I\,dl\right) \leqslant 1\,, \qquad (18)$$

where $n_2^{Xe}$, $n_2^{CaF_2}$, $n_2^{wg}$, and $n_2^{air}$ are nonlinear (depending on radiation intensity) refractive indices in Xe, calcium fluoride, working gas, and air, and $L_{Xe}$, $L_{CaF_2}$, $L_{wg}$, and $L_{air}$ are the corresponding propagation lengths. A xenon cell placed near the final amplifier, i.e., where filamentation had not yet formed, shifted its onset to a greater distance (see Fig. 14). The cell placed in a beam with already formed filaments effectively defocused them and leveled the energy distribution in the beam (Fig. 15). Note that defocusing of filaments due to diffraction also occurred in an empty evacuated cell, although to a significantly smaller degree than in xenon. A more detailed consideration of nonlinear processes during the amplification and propagation of UV laser beams with terawatt peak power is given in our review Ref. [190].

Filamentation of a UV laser beam in atmospheric air also has attractive aspects, since the extended plasma channels it creates can be used for highly directional transportation of powerful microwave radiation and initiation of atmospheric electrical discharges, including active protection against lightning discharges. As was shown in Ref. [191], the arrangement of an array of filaments can be controlled using amplitude masks, which makes it possible to form various plasma waveguide structures in atmospheric air. For example, a virtual hollow cylindrical tubular microwave waveguide with a plasma wall, operating due to the effect of total internal reflection of microwave radiation at grazing angles of incidence [192], or a slightly divergent plasma horn microwave antenna can be used for highly directional transmission of microwave radiation. The fundamental possibility of this approach was first demonstrated experimentally in our work (see Ref. [193]), where microwave radiation with a wavelength of 8 mm was captured in a diverging hollow tubular plasma horn with an opening angle of $\sim 1°$, which was formed in the air by a UV laser beam with an annular cross section (Fig. 16). The theory of grazing incidence plasma waveguides and

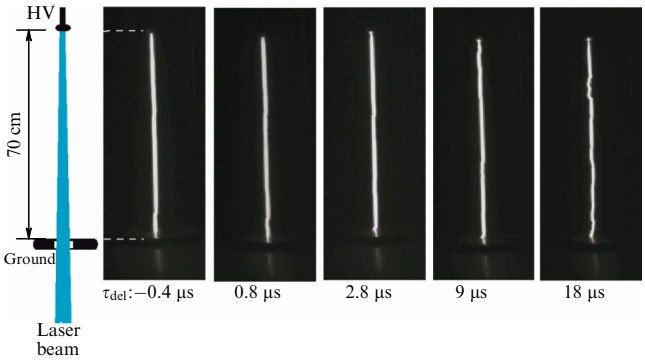


**Figure 17.** Images of a discharge initiated by an amplitude-modulated laser pulse in a 70-cm-long interelectrode gap for various delays between the laser pulse and a voltage pulse with an amplitude of 420 kV.

optimal conditions for their implementation using KrF lasers were considered in Refs [64, 194].

Effective control of the trajectory of $\sim$ 1-m-long electrical discharges in the air along plasma channels produced by focused smooth or amplitude-modulated 100-ns UV pulses was demonstrated in Refs [62, 63] (Fig. 17).

### 3.4 Repetition-rate excimer lasers

A start on the development of repetition-rate excimer lasers pumped by an electron beam and high average radiation power was made in the USA in 1977, after the possibility of scaling pulsed excimer facilities was demonstrated. The successful development of this work was facilitated by previous research and development on high-power gas-flow chemical lasers, which laid the foundations for the design of gas-dynamic circuits with a high quality gas flow. Already in 1980, the XeF laser facility EMRLDO was operational at MLI. In 1987, it was improved and, with a new gas-dynamic circuit, produced an average output power of 1 kW at wavelength $\lambda = 353$ nm at a pulse repetition rate of 100 Hz from a gain volume of $10 \times 10 \times 50$ cm, and with short-term operation it yielded 1.3 kW [195]. At a nominal pulse repetition rate of 40 Hz, the operating time of the installation was about 1 s. A higher-power EMRLD facility, which was made under the Strategic Defense Initiative (SDI) program of the US Department of Defense, was launched in 1989. At a pulse repetition rate of 100 Hz, it produced 4 kW of average power with a radiation divergence 1.3 times worse than the diffraction-limited one [196]. The main technical factor determining the duration of uninterrupted operation of the facility was the destruction of the foil window for extracting the electron beam from the vacuum diode into the laser chamber.

For repetition-rate KrF lasers intended for the driver of a fusion reactor, a lower pulse repetition rate (5–10 Hz) is required, but a very large number of pulses are required ($> 3 \times 10^8$) during non-stop operation of the LTF reactor for two years [75, 76]. Made at NRL within the framework of inertial thermonuclear fusion program (IFE) was the Electra repetition-rate KrF laser (see Fig. 9) [81, 197]. As a smaller prototype of the LTF driver, it was intended to test key technologies designed to increase the reliability of the main laser components and demonstrate the fundamental possibility of achieving the parameters required for the driver. To solve this problem, optimization of the composition and pumping of the working mixture was carried out [198, 199], as was numerical modeling of the kinetics of the gain medium using the Orestes program [200]. For long-term operation of vacuum diodes, solid-state power supplies [201, 202], new designs of cathodes, and a vacuum foil window with high transmittance for electron beams were developed [203]. The laser chamber of the main Electra KrF amplifier has dimensions of $30 \times 30 \times 100$ cm with a distance between optical windows of 135 cm. To pump the working mixture containing Kr, Ar, and $F_2$ at a pressure of 1–2 atm, use is made of two electron beams with a pulse duration of 140 ns stabilized by a permanent magnetic field. The circulation and cooling system of the working mixture produces a uniform gas flow in the laser chamber at a speed of 5–7 m s$^{-1}$, as well as forced cooling of the foil by the gas flow [204, 205]. In the oscillation mode, the laser operates with an output energy of up to 700 J at a pulse repetition rate of 5 Hz and a lifespan of 50,000 pulses [81, 206]. With two-pass amplification in an angular multiplexing scheme, Electra amplifies six 25-ns pulses to a total energy of 520 J [207].

An alternative approach to developing repetition-rate excimer lasers with high average output power is based on excitation of the gain medium by an electric discharge [208]. The absence of such a fragile structural element as a separating foil makes it possible to implement a high pulse repetition rate, up to 1 kHz, with a long service life. The main restrictions on the energy in a pulse are associated with a violation of the stability of the discharge in a large volume. However, the development of X-ray preionization has made it possible to significantly increase the volume of the gain medium of discharge-pumped lasers. Northlight, the largest repetition-rate discharge-pumped XeCl laser, had a volume of 36 l and produced an energy of 84 J [209]. At a repetition rate of 10 Hz, the laser could operate for 10 s, and at 5 Hz, for 3 min.

Developed at the Kurchatov Institute of Atomic Energy was a repetition-rate discharge-pumped XeCl laser with gas preionization by the UV radiation of a surface discharge, and the near-surface plasma simultaneously served as the plasma cathode of the main discharge [210]. From a gain volume of $10 \times 8 \times 80$ cm (6.4 l) at a working mixture pressure of 4 atm, single pulses with an energy of 12.7 J were obtained with an efficiency of $\sim$ 1%. In the repetition-rate mode with a pulse energy of $\sim$ 10 J and a repetition rate of 50 Hz, an average output laser power of 500 W was achieved. The divergence of radiation when using an unstable telescopic resonator with magnification $M = 12$ improved by 1–2 orders of magnitude compared to a plane resonator and amounted to 2–3 diffraction limits [211]. In this case, the laser energy decreased by only 30%.

Discharge-pumped excimer lasers with a relatively low energy of a few joules or fractions of a joule and a pulse duration of tens of nanoseconds, but a high pulse repetition rate of up to 1000 Hz, have been developed by a number of American, European, Japanese, and Russian laser centers and commercial firms. Such lasers are aimed primarily at medical and industrial applications and have a long service life and high reliability. Today, they are in greatest demand in ophthalmology, photolithography and display production. For many years, the leader in the development and production of such lasers was the Lambda Physik company (Germany), which in 2003 became part of the American company Coherent. The LPX 325i models commercially produced by this company with an average power of 120 W with XeCl and 160 W with KrF, the Lambda 3000 with a

power of 150 W with XeCl, had a guaranteed operating life of $10^9$ pulses. All these lasers are excited by an electrical discharge with UV preionization and magnetic compression of pump pulses. It was possible to obtain a higher energy and an average output power of 750 W during long-term operation at a pulse repetition rate of 500 Hz using a XeCl laser with X-ray preionization of the discharge [50].

The first repetition-rate XeCl discharge-pumped laser that reached an average radiation power of 1 kW was the SOPRA'VEL facility developed by SOPRA in France [51]. At a repetition rate of 80 to 100 Hz, the pulse energy ranged from 10 to 15 J. The pulse duration varied from 50 to 190 ns due to changes in the pressure and composition of the mixture, as well as the voltage applied to the discharge gap. To preionize the gain medium with a volume of $6 \times 8 \times 100$ cm, X-ray pulses with a duration of 400 ns were used. A double gas-dynamic circuit ensured a working gas flow velocity through the discharge gap of 18 m s$^{-1}$ at a gas pressure of up to 10 atm. With a maximum intrinsic efficiency of 2.6%, the total laser efficiency was 2%, taking into account the power of 1.5 kW consumed by each of the two centrifugal fans.

An XeCl excimer laser with a gain volume of $2.1 \times \times 2.5 \times 80$ cm, which was excited by a discharge with X-ray preionization, an average power of 1 kW, and a pulse repetition rate of 1 kHz, was developed jointly by the UK, Italy, and the Netherlands under the international Eureka program [212] . Similar work in Japan was coordinated by the Advanced Materials Processing and Technology Research Association (AMPTRA). These programs envisioned the development of industrial laser facilities with an average power of 2–10 kW.

### 3.5 Repetition-rate excimer laser systems for amplifying ultrashort pulses

Prior to the advent of titanium-sapphire lasers generating femtosecond ultrashort pulses, several methods were developed to produce seed ultrashort pulses of pico- and subpicosecond duration for subsequent amplification in excimer systems (see review [180]). To this end, advantage was most often taken of dye lasers with synchronous pumping by the second harmonic of mode-locked Nd:YAG or Ar lasers. The resultant picosecond pulses were passed through an optical fiber, where, due to self-phase modulation and group velocity dispersion, their spectrum was significantly broadened, and they were stretched in time and chirped in frequency. After this, the pulses were compressed to $\sim 100$ fs in an optical compressor formed by a pair of diffraction gratings. The resulting ultrashort pulses were amplified in several stages of dye amplifiers, then the radiation frequency was converted using nonlinear crystals into the UV region of the spectrum, into amplification bands of various excimers. For the KrF laser, this was achieved by sequential frequency doubling and mixing the harmonic and the fundamental frequency.

One of the first subterawatt KrF laser systems was made at the University of Illinois (USA) and generated 600-fs radiation pulses with an energy of 0.25 J at a repetition rate of 0.4 Hz [181]. A discharge-pumped amplifier with a length of 2.5 m, aperture of $10 \times 10$ cm, and X-ray preionization was used as the output stage. This system reached a record intensity of $2 \times 10^{19}$ W cm$^{-2}$ when focusing radiation with a parabolic mirror onto a spot with a diameter of less than 1.7 μm. A similar repetitively pulsed terawatt KrF laser system, but operating at a higher pulse repetition rate of 10 Hz, was made at the Institute of Solid State Physics of the University of Tokyo [213]. After the output stage — a discharge-pumped amplifier with UV preionization and an aperture of $6 \times 4$ cm — the USP energy ranged up to 0.4 J with a duration of 280 fs. When focusing radiation, the intensity in the focal spot with a diameter of 2 μm exceeded $2 \times 10^{19}$ W cm$^{-2}$.

The shortest duration of ultrashort pulses, 80 fs, was obtained at the Max Planck Institute for Biophysical Chemistry (Germany), where they were formed using an even more complex method based on a gradual reduction in duration while amplifying ultrashort pulses in dyes in configurations with a quenched resonator, a short resonator, and a resonator with distributed feedback [214].

Hybrid laser systems with a Ti:sapphire generator of femtosecond ultrashort pulses and conversion of the radiation frequency into the amplification band of KrF discharge-pumped amplifiers have not only significantly simplified the arrangement and operation of laser systems, but also significantly expanded the range of parameters. For instance, at the Institute of Solid State Physics (Japan), several repetition-rate ultrashort-pulse laser systems were developed. One of them generated terawatt peak powers of USPs with a repetition rate of 10 Hz [215]; the other generated USPs with a repetition frequency of 1 kHz and an average output power of 7 W [216]. The highest average power of 50 W was achieved at a USP repetition rate of 200 Hz [217].

## 4. Conclusions

The implementation of a laser based on bound-free electronic transitions of liquefied xenon at the Laboratory of Quantum Radiophysics of the Lebedev Physical Institute under the leadership of Academician N G Basov was the beginning of a new direction in the development of high-power excimer laser systems operating in the visible, UV, and VUV ranges. As follows from the review presented, a number of priority research studies on excimer lasers pumped by an electron beam, carried out at the Lebedev Physical Institute in the 1970–1980s, contributed to a detailed understanding of the kinetic processes in the gain media of various excimer lasers and initiated similar research and development at universities, research centers, and industrial firms in many countries. In the USA, by the early 1980s, excimer lasers based on noble gas halides with a large gain volume of tens and hundreds of liters and a laser energy of hundreds of joules were launched. Research at these facilities demonstrated the possibility of their further scaling and stimulated the development of the necessary element base. Technologies were developed for generating high-current relativistic electron beams of large cross-section required to excite large volumes of the gain medium; pulsed high-voltage power supply systems for electron accelerators, gas-dynamic circuits for circulating the working mixture, and a technology for manufacturing high-quality optical elements for the UV region of the spectrum were developed. Government programs financed the development of high-power excimer lasers for military applications, LTF, isotope separation, etc., which made it possible by the mid-1980s to make a number of unique pulsed laser systems with an energy up to 10 kJ, close to diffraction-limited radiation divergence, as well as systems of repetition-rate operation with an average power of several kilowatts for military and industrial applications. Very detailed designs of KrF laser drivers with energies above 1 MJ for LTF were developed. Work on the development of repetition-rate

discharge-pumped excimer lasers with an average output power of hundreds of watts and a long operating life in European countries, the USA, and Japan was making rapid strides for use in medicine, photolithography, and microelectronics. Before the advent of the principles of amplification of chirped pulses in solid-state systems, until the 1990s, USP excimer amplifiers provided record terawatt peak powers in sub-picosecond pulses and radiation intensities of $\sim 10^{19}$ W cm$^{-2}$ in a focused beam. Many of the listed applications have remained relevant to this day, and some of them show good promise for future developments, for example, as KrF laser drivers for LTF power plants, active lightning protection systems, and highly directional transmission of microwave radiation through virtual plasma waveguides.

The main contributor to the development of excimer lasers in our country, in addition to the Lebedev Physical Institute, was the Institute of High-Current Electronics in Tomsk, where pulsed excimer lasers with laser energies of hundreds of joules were launched and fundamentally new power supplies for electron accelerators for electron beam or photodissociation pumping were developed, and also the Kurchatov Institute of Atomic Energy, where the highest average output power of up to 1 kW was obtained using repetition-rate discharge-pumped excimer lasers. The GARPUN multifunctional KrF laser system was made in 1991 on the initiative of N G Basov in the Quantum Radiophysics Division of the Lebedev Physical Institute. Second in scale to the largest excimer laser systems in the world, today it is the only world-class facility in Russia, which makes it possible to conduct research in a wide range of areas, including LTF, high energy density physics, and various applied problems.

**Acknowledgments**

The author expresses his appreciation to A A Ionin, A O Levchenko, L V Seleznev, D V Sinitsyn, I V Smetanin, A V Shutov, I V Kholin, and N N Ustinovskii for many years of fruitful cooperation.

This work was supported by the Russian Science Foundation under grant no. 22-22-01021.

## References

1. Houtermans F G *Helv. Phys. Acta* **33** 933 (1960)
2. Basov N G "Opening remarks", in *Forth Intern. Quantum Electronics Conf., Phoenix, AZ, April 12–15, 1966*; *IEEE J. Quantum Electron.* **2** 354 (1966)
3. Basov N G et al. *Kratk. Soobshch. Fiz. FIAN* (8) 10 (1970)
4. Basov N G et al. *JETP Lett.* **12** 329 (1970); *Pis'ma Zh. Eksp. Teor. Fiz.* **12** 473 (1970)
5. Koehler H A et al. *Appl. Phys. Lett.* **21** 198 (1972)
6. Gerardo J M, Johnson A W *IEEE J. Quantum Electron.* **9** 748 (1973)
7. Hoff P W, Swingle J C, Rhodes C K *Appl. Phys. Lett.* **23** 245 (1973)
8. Hughes W M, Shannon J, Hunter R *Appl. Phys. Lett.* **24** 488 (1974)
9. Molchanov A G *Sov. Phys. Usp.* **15** 124 (1972); *Usp. Fiz. Nauk* **106** 165 (1972)
10. Eletskii A V *Sov. Phys. Usp.* **21** 502 (1978); *Usp. Fiz. Nauk* **125** 279 (1978)
11. Lakoba I S, Yakovlenko S I *Sov. J. Quantum Electron.* **10** 389 (1980); *Kvantovaya Elektron.* **7** 677 (1980)
12. Rhodes Ch K (Ed.) *Excimer Lasers* (Berlin: Springer-Verlag, 1979); Translated into Russian: *Eksimernye Lazery* (Moscow: Mir, 1981)
13. Smirnov B M *Sov. Phys. Usp.* **26** 31 (1983); *Usp. Fiz. Nauk* **139** 53 (1983)
14. Molchanov A G *Trudy Fiz. Inst. Akad. Nauk* **171** 54 (1986); *Proc. Lebedev Phys. Inst.* **171** 72 (1988)
15. McDaniel E W, Nighan W L (Eds) *Gas Lasers* (New York: Academic Press, 1982); Translated into Russian: *Gazovye Lazery* (Moscow: Mir, 1986)
16. Slade P D, Fournier G R *Opt. Commun.* **29** 325 (1979)
17. Gold M G, Thrush B A *Chem. Phys. Lett.* **29** 486 (1974)
18. Velazco J E, Setser D W *J. Chem. Phys.* **62** 1990 (1975)
19. Brau C A, Ewing J J *Appl. Phys. Lett.* **27** 435 (1975)
20. Ewing J J, Brau C A *Appl. Phys. Lett.* **27** 350 (1975)
21. Searles S K, Hart G A *Appl. Phys. Lett.* **27** 243 (1975)
22. Hoffman J M, Hays A K, Tisone G C *Appl. Phys. Lett.* **28** 538 (1976)
23. Murray J R, Powell H T *Appl. Phys. Lett.* **29** 252 (1976)
24. Mangano J A, Jacob J H *Appl. Phys. Lett.* **27** 495 (1975)
25. Burnham R, Powell F X, Djeu N *Appl. Phys. Lett.* **29** 30 (1976)
26. Wang C P et al. *Appl. Phys. Lett.* **28** 326 (1976)
27. Burnham R, Djeu N *Appl. Phys. Lett.* **29** 707 (1976)
28. Sumida S, Obara M, Fujioka T *Appl. Phys. Lett.* **33** 913 (1978)
29. Basov N G et al. *Sov. Tech. Phys. Lett.* **11** 433 (1985); *Pis'ma Zh. Tekh. Fiz.* **11** 1044 (1985)
30. Eden J G et al. *Appl. Phys. Lett.* **35** 133 (1979)
31. Krotz W et al. *Appl. Phys. Lett.* **55** 2265 (1989)
32. Adonin A et al. *Laser Part. Beams* **27** 379 (2009)
33. Christensen C P, Waynant R W *Appl. Phys. Lett.* **41** 794 (1982)
34. Mendelsohn A J et al. *Appl. Phys. Lett.* **38** 603 (1981)
35. Didenko A N et al. *Pis'ma Zh. Tekh. Fiz.* **12** 1245 (1986)
36. Hill R M et al. *Appl. Phys. Lett.* **34** 137 (1979)
37. Bischel W K et al. *Appl. Phys. Lett.* **34** 565 (1979)
38. Basov N G et al. *Sov. J. Quantum Electron.* **6** 505 (1976); *Kvantovaya Elektron.* **3** 930 (1976)
39. Basov N G et al. *Sov. J. Quantum Electron.* **7** 1401 (1977); *Kvantovaya Elektron.* **4** 2453 (1977)
40. Basov N G et al. *Sov. J. Quantum Electron.* **9** 629 (1979); *Kvantovaya Elektron.* **6** 1074 (1979)
41. Schwentner N, Apkarian V A *Chem. Phys. Lett.* **154** 413 (1989)
42. Katz A I, Feld J, Apkarian V A *Opt. Lett.* **14** 441 (1989)
43. Smiley V N *Proc. SPIE* **1225** 2 (1990)
44. Rosocha L A et al. *Laser Part. Beams* **4** 55 (1986)
45. Rosocha L A et al. *Fusion Technol.* **11** 497 (1987)
46. Sullivan J A, Von Rosenberg C W (Jr.) *Laser Part. Beams* **4** 91 (1986)
47. Sullivan J A *Fusion Technol.* **11** 684 (1987)
48. Champagne L F, Dudas A J, Harris N W *J. Appl. Phys.* **62** 1567 (1987)
49. Walter R F et al. *Proc. SPIE* **1397** 71 (1990)
50. Muller-Horsche E, Osterlin P, Bastling D *Proc. SPIE* **1225** 142 (1990)
51. Godard B et al., in *Conf. on Lasers and Electrooptics CLEO-93, Baltimore, MD, May 2–7, 1993*, Paper CTh1
52. Zvorykin V D et al. *Proc. SPIE* **5120** 223 (2003)
53. Zvorykin V D et al. *Plasma Fusion Res.* **8** 3405046 (2013)
54. Zvorykin V D et al. *Laser Part. Beams* **19** 609 (2001)
55. Zvorykin V D et al. *Laser Part. Beams* **25** 435 (2007)
56. Ewing J J et al. *IEEE J. Quantum Electron.* **15** 368 (1979)
57. Lowenthal D D et al. *IEEE J. Quantum Electron.* **17** 1861 (1981)
58. Tilleman M M, Jacob J H *Appl. Phys. Lett.* **50** 121 (1987)
59. Zvorykin V D, Lebo I G, Rozanov V B *Kratk. Soobshch. Fiz. FIAN* (9–10) 20 (1997)
60. Zvorykin V D et al. *Quantum Electron.* **43** 332 (2013); *Kvantovaya Elektron.* **43** 332 (2013)
61. Betti R et al. *Phys. Rev. Lett.* **98** 155001 (2007)
62. Zvorykin V D et al. *Quantum Electron.* **43** 339 (2013); *Kvantovaya Elektron.* **43** 339 (2013)
63. Zvorykin V D et al. *Plasma Phys. Rep.* **41** 112 (2015); *Fiz. Plazmy* **41** 125 (2015)
64. Zvorykin V D et al. *Appl. Opt.* **53** I31 (2014)
65. Robertson K L, Avicola K *Proc. SPIE* **1225** 44 (1990)
66. Smith M J, Trainor D W, Duzy C *IEEE J. Quantum Electron.* **26** 942 (1990)
67. Nicholson B W et al. *IEEE J. Quantum Electron.* **26** 1285 (1990)
68. Swingle J C et al. *J. Appl. Phys.* **52** 91 (1981)
69. Murray J R et al. *IEEE J. Quantum Electron.* **15** 342 (1979)
70. Schlitt L, in *2nd IEEE Intern. Pulsed Power Conf. Digest of Papers, Lubbock, Texas. 1979*, p. 269
71. Bigio I J, Slatkine M *IEEE J. Quantum Electron.* **19** 1426 (1983)

72. Turnur T P et al. *Proc. SPIE* **1225** 23 (1990)
73. Harris D B et al. *Fusion Technol.* **11** 705 (1987)
74. Hunter A M *IEEE J. Quantum Electron.* **22** 386 (1986)
75. Sviatoslavsky I N et al. *Fusion Technol.* **21** 1470 (1992)
76. Von Rosenberg C W (Jr.) *Fusion Technol.* **21** 1600 (1992)
77. Harris D B et al. *Laser Part. Beams* **11** 323 (1993)
78. Obenschain S P et al. *Phys. Plasmas* **3** 2098 (1996)
79. Lehmberg R H, Goldhar J *Fusion Sci. Technol.* **11** 532 (1987)
80. Lehmberg R H, Schmitt A J, Bodner S E *J. Appl. Phys.* **62** 2680 (1987)
81. Obenschain S et al. *Appl. Opt.* **34** F103 (2015)
82. Deniz A V, Obenschain S P *Opt. Commun.* **106** 113 (1994)
83. Pronko M S *IEEE J. Quantum Electron.* **30** 2147 (1994)
84. Lehecka T et al. *Opt. Commun.* **117** 485 (1995)
85. Deniz A V et al. *Opt. Commun.* **147** 402 (1998)
86. Pawley C J et al. *Phys. Plasmas* **4** 1969 (1997)
87. Pawley C J et al. *Fusion Eng. Des.* **44** 171 (1999)
88. Weaver J L et al. *Phys. Plasmas* **14** 056316 (2007)
89. Karasik M et al. *Phys. Plasmas* **17** 056317 (2010)
90. Aglitskiy Y et al. *Phys. Rev. Lett.* **109** 085001 (2012)
91. Weaver J L et al. *Phys. Plasmas* **20** 022701 (2013)
92. Karasik M et al. *Phys. Rev. Lett.* **114** 085001 (2015)
93. Zulick C et al. *Phys. Plasmas* **27** 072706 (2020)
94. Sethian J D et al. *IEEE Trans. Plasma Sci.* **38** 1690 (2010)
95. Bodner S E, Schmitt A J, Sethian J D *High Power Laser Sci. Eng.* **1** 2 (2013)
96. Kehne D M et al. *Rev. Sci. Instrum.* **84** 013509 (2013)
97. Igumenshchev I V et al. *Phys. Rev. Lett.* **110** 145001 (2013)
98. Sethian J D et al. *Fusion* **43** 1693 (2003)
99. Sethian J D et al. *Proc. IEEE* **92** 1043 (2004)
100. Stamper J A et al. *Nucl. Fusion* **44** 745 (2004)
101. Myers M C et al. *Nucl. Fusion* **44** S247 (2004)
102. Obenschain S P et al. *Phys. Plasmas* **13** 056320 (2006)
103. Schmitt A J et al. *Fusion Sci. Technol.* **56** 377 (2009)
104. Obenschain S P, Sethian J D, Schmitt A J *Fusion Sci. Technol.* **56** 594 (2009)
105. Schmitt A J et al. *Phys. Plasmas* **17** 042701 (2010)
106. Shcherbakov V A *Sov. J. Plasma Phys.* **9** 240 (1983); *Fiz. Plazmy* **9** 409 (1983)
107. Lindl J *Phys. Plasmas* **2** 3933 (1995)
108. Lehmberg R H, Giuliani J L, Schmitt A J *J. Appl. Phys.* **106** 023103 (2009)
109. Abu-Shawareb H et al. (Indirect Drive ICF Collab.) *Phys. Rev. Lett.* **129** 075001 (2022)
110. Zylstra A B et al. *Phys. Rev. E* **106** 025202 (2022)
111. National Ignition Facility achieves fusion ignition, https://llnl.gov/news/national-fusion-facility-achievs ignition; DOE National Laboratory Makes History by Achieving Fusion Ignition, https://energy.gov/articles/doe-national-laboratory-makes-history-achieving-fusion-ignition
112. Temporal M et al. *High Power Laser Sci. Eng.* **2** e8 (2014)
113. Galakhov I V et al. *Fusion Eng. Des.* **44** 51 (1999)
114. Garanin S G, Krokhin O N *Herald Russ. Acad. Sci.* **81** 204 (2011); *Vestn. Ross. Akad. Nauk* **81** 495 (2011)
115. He X T et al. *Fusion Eng. Des.* **44** 57 (1999)
116. Zheng W et al. *High Power Laser Sci. Eng.* **4** e21 (2016)
117. Gong T et al. *Matter Radiat. Extremes* **4** 055202 (2019)
118. Erlandson A C et al. *Opt. Mater. Express* **1** 1341 (2011)
119. Edwards C B, Danson C N *High Power Laser Sci. Eng.* **3** e4 (2015)
120. Suda A, Obara M, Noguchi A *J. Appl. Phys.* **60** 3791 (1986)
121. Wolford M F et al. *High Energy Density Phys.* **36** 100801 (2020)
122. Bodner S E *High Power Laser Sci. Eng.* **7** e63 (2019)
123. Obenschain S P *Philos. Trans. R. Soc. A* **378** 20200031 (2020)
124. Edwards C B et al. *AIP Conf. Proc.* **100** 59 (1983)
125. Barr J R M et al. *Opt. Commun.* **66** 127 (1988)
126. Partanen J P, Shaw M J *J. Opt. Soc. Am. B* **3** 1374 (1986)
127. Shaw M J et al. *J. Opt. Soc. Am. B* **3** 1466 (1986)
128. Hooker C J, Lister J M D, Rodgers P A *Opt. Commun.* **82** 497 (1991)
129. Shaw M J et al. *Opt. Lett.* **16** 1320 (1993)
130. Shaw M J *Laser Part. Beams* **9** 309 (1991)
131. Shaw M J et al. *Laser Part. Beams* **11** 331 (1993)
132. Divall E J et al. *J. Mod. Opt.* **43** 1025 (1996)
133. Shaw M J et al. *Fusion Eng. Des.* **44** 209 (1999)
134. Foldes I B, Szatmari S *Laser Part. Beams* **26** 475 (2008)
135. Tabak M et al. *Phys. Plasmas* **1** 1626 (1994)
136. Tabak M et al. *Phys. Plasmas.* **12** 057305 (2005)
137. Gus'kov S Yu *Fiz. Plazmy* **39** 3 (2013)
138. Kim Y P, Hutchinson M H R *Appl. Phys. B* **49** 469 (1989)
139. Ross I N et al. *J. Mod. Opt.* **37** 555 (1990)
140. Martin W E, Winfield R J *Appl. Opt.* **27** 567 (1988)
141. Strickland D, Mourou G *Opt. Commun.* **56** 219 (1985)
142. Houliston J R et al. *Opt. Commun.* **104** 350 (1994)
143. Ross I N et al. *Opt. Commun.* **109** 288 (1994)
144. Owadano Y et al. *Laser Part. Beams* **7** 383 (1989)
145. Owadano Y et al. *Laser Part. Beams* **11** 347 (1993)
146. Tanimoto M et al. *Laser Part. Beams* **4** 71 (1986)
147. Tomie T et al. *Laser Part. Beams* **8** 299 (1990)
148. Okuda I et al. *Fusion Eng. Des.* **44** 377 (1999)
149. Owadano Y et al. *Fusion Eng. Des.* **44** 91 (1999)
150. Owadano Y et al., in *Inertial Fusion Sciences and Applications 2001* (Eds K A Tanaka, D D Meyerhofer, J Meyer-ter-Vehn) (Amsterdam: Elsevier, 2001) p. 465
151. Matsumoto Y et al. *Fusion Eng. Des.* **44** 383 (1999)
152. Takahashi E et al. *Fusion Eng. Des.* **44** 133 (1999)
153. Ueda K *Laser Part. Beams* **7** 375 (1989)
154. Sasaki A et al. *J. Appl. Phys.* **65** 231 (1989)
155. Ueda K et al. *Laser Part. Beams* **11** 31 (1993)
156. Nishioka H et al. *Opt. Lett.* **14** 692 (1989)
157. Watanabe S et al. *J. Opt. Soc. Am. B* **6** 1870 (1989)
158. Wang N et al. *Laser Part. Beams* **20** 119 (2002)
159. Shan Y et al. *Laser Part. Beams* **20** 123 (2002)
160. Xiang Y *Proc. SPIE* **6279** 62795Z (2007)
161. Gao Z *Proc. SPIE* **8796** 87961R (2013)
162. Zhao X et al. *Proc. SPIE* **9255** 925523 (2015)
163. Zhang Y et al. *Proc. SPIE* **9543** 95431C (2015)
164. Basov N G et al. *Pis'ma Zh. Tekh. Fiz.* **8** 245 (1982)
165. Baranov V Yu et al. *Pis'ma Zh. Tekh. Fiz.* **9** 201 (1983)
166. Bychkov Yu I et al. *Sov. J. Quantum Electron.* **17** 605 (1987); *Kvantovaya Elektron.* **14** 953 (1987)
167. Bychkov Yu I et al. *Pis'ma Zh. Tekh. Fiz.* **14** 566 (1988)
168. Abdullin E N et al. *Quantum Electron.* **23** 564 (1993); *Kvantovaya Elektron.* **20** 652 (1993)
169. Bugaev S P et al. *Sov. J. Quantum Electron.* **34** 801 (2004); *Kvantovaya Elektron.* **34** 801 (2004)
170. Aristov A I et al. *Opt. Atmos. Okeana* **22** 1029 (2009)
171. Bychkov Yu I et al. *Sov. J. Quantum Electron.* **17** 605 (1987); *Kvantovaya Elektron.* **43** 190 (2013)
172. Alekseev S V et al. *Izv. Vyssh. Uchebn. Zaved.* **62** (11) 178 (2019)
173. Basov N G et al. *Sov. J. Quantum Electron.* **21** 816 (1991); *Kvantovaya Elektron.* **18** 902 (1991)
174. Arlantsev S V et al. *Quantum Electron.* **24** 223 (1994); *Kvantovaya Elektron.* **21** 241 (1994)
175. Basov N G et al. *J. Sov. Laser Res.* **14** 326 (1993)
176. Basov N G et al. *Quantum Electron.* **21** 13 (1994); *Kvantovaya Elektron.* **21** 15 (1994)
177. Zvorykin V D et al. *Laser Part. Beams* **19** 609 (2001)
178. Zvorykin V D et al. *Laser Part. Beams* **25** 435 (2007)
179. Zvorykin V D, Levchenko A O, Ustinovskii N N *Quantum Electron.* **40** 381 (2010); *Kvantovaya Elektron.* **40** 381 (2010)
180. McIntyre I A, Rhodes C K *J. Appl. Phys.* **69** R1 (1991)
181. Luk T S et al. *Opt. Lett.* **14** 1113 (1989)
182. Couairon A, Mysyrowicz A *Phys. Rep.* **47** 441 (2007)
183. Smetanin I V et al. *Nucl. Instrum. Meth. Phys. Res. B* **369** 87 (2016)
184. Shutov A V *Appl. Phys. Lett.* **111** 224104 (2017); *Appl. Phys. Lett.* **113** 189902 (2018) Erratum
185. Shipilo D E et al. *Opt. Express* **25** 25386 (2017)
186. Zvorykin V D et al. *J. Opt. Soc. Am. B* **36** G25 (2019)
187. Zvorykin V D et al. *Nucl. Instrum. Meth. Phys. Res. B* **355** 227 (2015)
188. Zvorykin V D et al. *Quantum Electron.* **44** 431 (2014); *Kvantovaya Elektron.* **44** 431 (2014)
189. Zvorykin V D et al. *Laser Phys. Lett.* **13** 125404 (2016)
190. Zvorykin V D et al. *Matter Radiat. Extremes* **5** 045401 (2020)
191. Zvorykin V D et al. *Nucl. Instrum. Meth. Phys. Res. B* **402** 331 (2017)
192. Askar'yan G A *Sov. Phys. JETP* **1** 162 (1965); *Pis'ma Zh. Eksp. Teor. Fiz.* **1** 18 (1965)
193. Zvorykin V D et al. *Kratk. Soobshch. Fiz. FIAN* (2) 49 (2010)

194. Zvorykin V D et al. *Phys. Plasmas* **19** 033509 (2012)
195. Zahnow C F, in *Intern. Congress Opt. Sci. Eng. Humburg, Germany, September, 1988*, p. 56, Paper 1023-09
196. Walter R F et al. *Proc. SPIE* **1397** 71 (1990)
197. Wolford M F et al. *Appl. Phys. Lett.* **84** 326 (2004)
198. Hegeler F et al. *Phys. Plasmas* **11** 5010 (2004)
199. Petrov G M, Giuliani J L, Dasgupta A *J. Appl. Phys.* **91** 2662 (2002)
200. Lehmberg R H, Giuliani J L *J. Appl. Phys.* **94** 31 (2003)
201. Sethian J D *IEEE Trans. Plasma Sci.* **28** 1333 (2000)
202. Hegeler F et al. *IEEE Trans. Dielectr. Electr. Insul.* **18** 1205 (2011)
203. Friedman M et al. *J. Appl. Phys.* **95** 2797 (2004)
204. Lu B et al. *J. Fusion Energy* **30** 453 (2011)
205. Lu B et al. *Fusion Eng. Des.* **87** 352 (2012)
206. Wolford M F et al. *Proc. SPIE* **6454** 645407 (2007)
207. Wolford M F et al. *Opt. Eng.* **47** 104202 (2008)
208. Burnham R, Djeu N *Appl. Phys. Lett.* **29** 707 (1976)
209. Tillotson J M, in *SPIE Intern. Conf. on Lasers' 88, Lake Tahoe, NV, December 4–9, 1988*, Paper H1.2
210. Borisov V M et al. *Sov. J. Quantum Electron.* **17** 123 (1990); *Kvantovaya Elektron.* **17** 164 (1990)
211. Baranov V Yu et al. *Sov. J. Quantum Electron.* **18** 1065 (1988); *Kvantovaya Elektron.* **15** 1712 (1988)
212. Heman W J W et al. *Proc. SPIE* **1225** 132 (1990)
213. Watanabe S et al., in *Intern. Quantum Electronics Conf. CLEO-90/IQEC-90, Anaheim, Cal, May 24–28, 1990*, Paper JMA4
214. Szatmári S et al. *Opt. Commun.* **63** 305 (1987)
215. Nabekawa Y et al. *Opt. Lett.* **18** 1922 (1993)
216. Nabekawa Y et al. *Opt. Lett.* **21** 647 (1996)
217. Nabekawa Y et al. *Opt. Lett.* **26** 807 (2001)